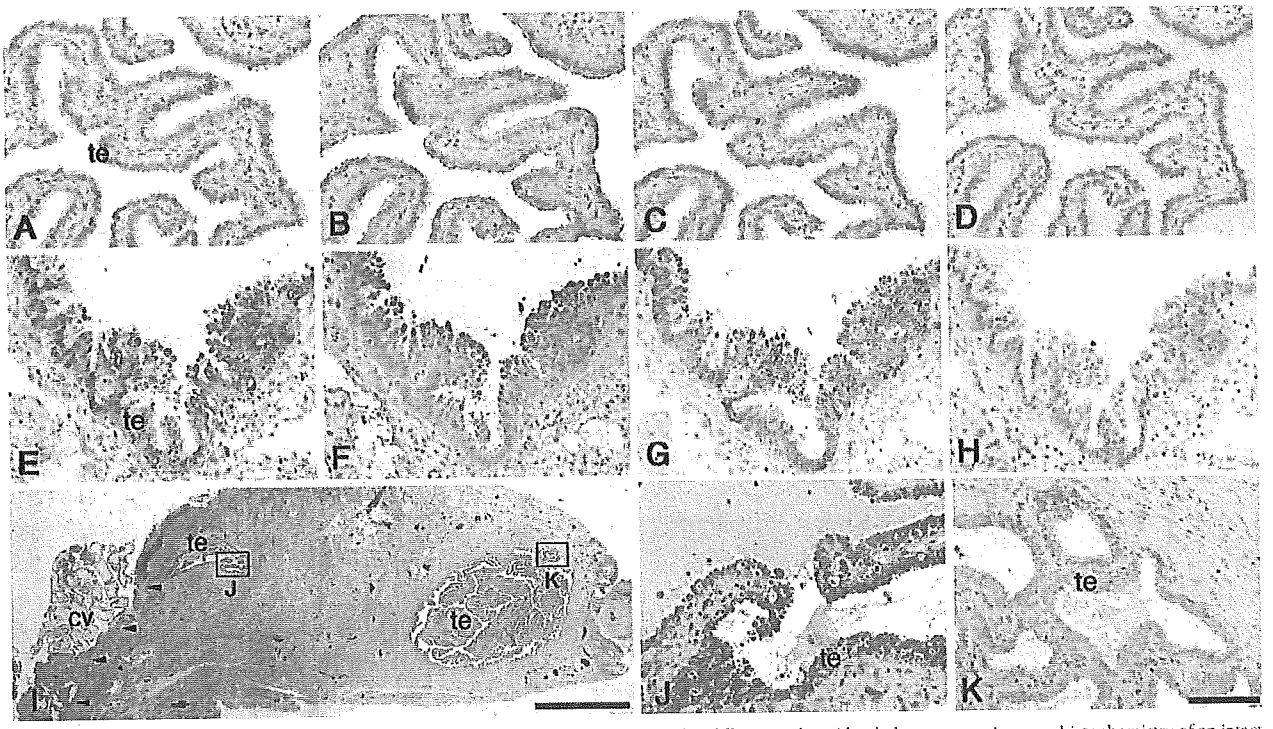

Figure 2. Expression of trophinin, tastin, and bystin proteins in intact fallopian tube and in fallopian tube with tubal pregnancy. Immunohistochemistry of an intact fallopian tube (**A–D**) and a fallopian tube with tubal pregnancy (**E–K**) for trophinin (**A, E, J, K**), tastin (**B, F**), and bystin (**C, G**). Hematoxylin and eosin-stained specimen from a tubal pregnancy (**I**), and high magnification of insets showing immunohistochemistry for trophinin in the area close to (**J**) or distant from (**K**) the chorionic villi. The implantation site in (**I**) is marked by **arrowheads**. All photographs except (**I**) are in the same magnification, and the **bar** in (**K**) indicates 100 μm. **Bar** in (**I**) indicates 2.0 mm. (cv, chorionic villi; te, tubal epithelia).

Overexpression of Trophinin Protein in Maternal Epithelial Cells in Tubal Pregnancy

Immunohistochemistry of intact fallopian tubes from non-pregnant and *in utero* pregnant women showed barely detectable levels of trophinin protein in tubal epithelial cells (Figure 2A, Table 1). On the other hand, various amounts of tastin and bystin proteins were detected in the cilia and the cytoplasm of the intact fallopian tube epithelia, respectively, regardless of non-pregnancy or *in utero* pregnancy (Figure 2, B and C, Table 1).

The signals for trophinin protein in tubal epithelia adjacent to the implantation site of tubal pregnancies were remarkably higher (Figure 2E) than those in intact fallopian tubes (Figure 2A, Table 2). Trophinin proteins were found in the cytoplasm of tubal epithelia with large apical protrusions or pinopodes (Figure 2E). Strong signals for tastin and bystin proteins were also seen in tubal epithelia with tubal pregnancies (Figure 2, F and G, Table 2). The levels of tastin and bystin appear to be elevated in association with ectopic pregnancy compared to those seen in intact fallopian tubes (Tables 1 and 2).

In addition, we also found that within a specimen of tubal pregnancy (Figure 2I), maternal epithelia close to the chorionic villi showed a stronger signal for trophinin (Figure 2J) than epithelial cells distant from the chorionic villi (Figure 2K). Similar observations that strong signals for trophinin were detected in the maternal endometrial glandular epithelial cells adjacent to the chorionic villi were made previously in human placenta from early pregnancy.[15] These results suggest the possibility that an embryonic factor functions locally to induce trophinin expression in maternal cells.

Expression of Trophinin Transcripts by Maternal Cells in Tubal Pregnancy

To confirm the results obtained by immunohistochemistry, we compared levels of trophinin, tastin, and bystin transcripts in non-pregnancy, *in utero* pregnancy and tubal pregnancy by *in situ* hybridization. Thus we examined three intact fallopian tubes from patients unrelated to tubal pregnancy and three fallopian tubes from tubal pregnancies. The results showed that levels of trophinin transcripts in the fallopian tube epithelia from tubal pregnancies were higher than those seen in intact fallopian tubes from *in utero* pregnancies or non-pregnancies (Figure 3A and G). We also observed that signals for trophinin transcripts are strong in the maternal epithelia adjacent to the chorionic villi, whereas epithelia far from the chorionic villi barely express trophinin transcripts (data not shown). These observations suggest that trophinin expression by maternal cells is induced by tubal pregnancy. By contrast, although the expression levels of tastin and bystin mRNAs were slightly increased in tubal pregnancy (Figure 3, B, C, H, and I), these differences in tastin and bystin transcripts between intact fallopian tubes and the fallopian tubes from tubal pregnancies were not as significant as those observed for trophinin.

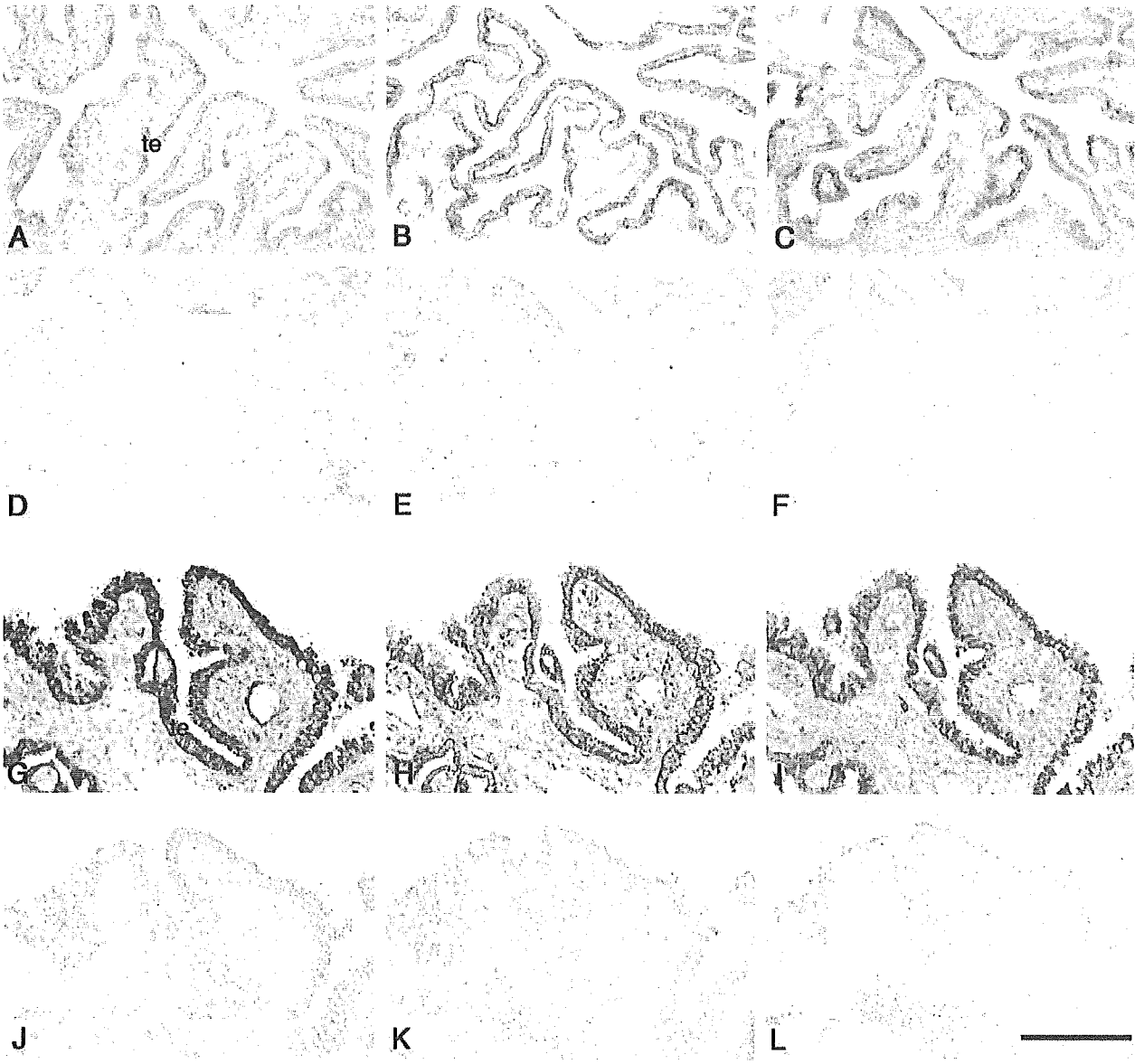

Figure 3. Expression of trophinin, tastin, and bystin transcripts in intact fallopian tube and in that with tubal pregnancy. *In situ* hybridization of an intact fallopian tube (**A–F**), and a fallopian tube with tubal pregnancy (**G–L**) for trophinin (**A** and **G**, antisense; **D** and **J**, sense), tastin (**B** and **H**, antisense; **E** and **K**, sense), and bystin (**C** and **I**, antisense; **F** and **L**, sense) using digoxigenin-labeled RNA probes. All photographs presented are in the same magnification, and the **bar** in (**L**) indicates 200 μm. (te, tubal epithelia).

Induction of Trophinin by hCG in Fallopian Tubal Epithelial Cells

Trophinin was barely detectable in intact fallopian tubes, regardless of whether they were derived from pregnant or non-pregnant patients (Figure 2A, Table 1). This observation suggests that steroid hormones associated with pregnancy are unlikely to promote strong trophinin expression in the tubal epithelial cells.

Since it is known that the trophectoderm cells of preimplantation embryo and chorionic villi trophoblasts secrete hCG,[21–24] we determined if hCG induces trophinin expression by maternal cells. On incubation of explants of the intact fallopian tube with hCG at 100 IU/ml for 24 hours, levels of trophinin proteins were significantly increased (Figure 4, A and E). No differences were found in the response to hCG among fallopian tubal explants regardless of whether they were derived from the region close to or far from the uterus. The explants incubated with lower concentrations of hCG (10 IU/ml) also showed elevation of trophinin protein, but at lower levels than at 100 IU/ml (data not shown). On the other hand, significant amounts of tastin and bystin were expressed in intact fallopian tubes (Figure 4, B and C), and their levels were not significantly altered by incubation with hCG (Figure 4, F and G).

To examine whether hCG induces the expression of trophinin at the transcriptional level, we determined the quantity of trophinin mRNA in the explants of intact fallopian tube by a real-time RT-PCR method. Thus the fallo-

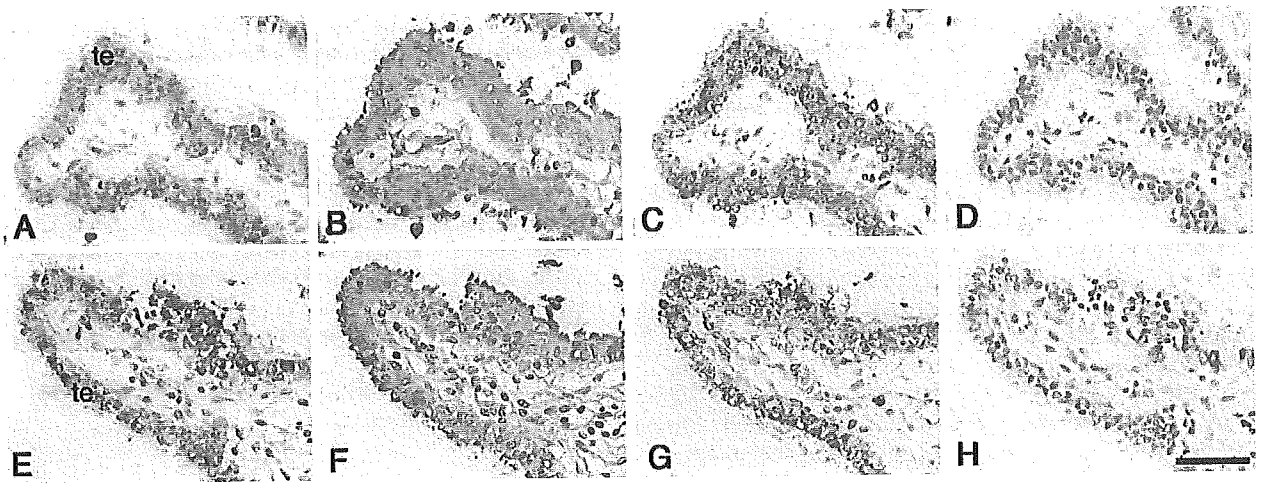

Figure 4. Comparison of trophinin, tastin, and bystin proteins in explants of intact fallopian tube with or without incubation with hCG. Explants were cultured for 24 hours without hCG (**A–D**) or with 100 IU/ml hCG (**E–H**), and were immunostained for trophinin (**A, E**), tastin (**B, F**), bystin (**C, G**), and second antibody alone (**D, H**). All photographs presented are in the same magnification, and the **bar** in (**H**) indicates 50 μm. (te, tubal epithelia).

pian tube specimens isolated from two patients unrelated to the ectopic pregnancy were incubated with hCG, and the quantities of trophinin mRNA were compared with those without hCG. In both experiments, trophinin transcripts in the explants increased in a dose-dependent manner of hCG (Table 3). These results strongly suggest that hCG induces the expression of trophinin gene by the fallopian tube epithelia.

Discussion

In this study, we found that trophinin, tastin, and bystin are expressed strongly in the trophoblasts and in maternal epithelia during ectopic tubal pregnancy (Figures 1, 2, and 3, Table 2). Expression patterns of these molecules in tubal pregnancy are similar to those seen in placenta during *in utero* pregnancy.[15] Thus the trophoblasts of chorionic villi and the maternal epithelia adjacent to chorionic villi strongly express trophinin, tastin, and bystin. One intriguing finding in this study is that the intact fallopian tubes isolated from women with *in utero* pregnancy express negligible levels of trophinin (Table 1). This finding indicates that steroid hormones alone cannot induce strong trophinin expression in humans. Furthermore, the results suggest the existence of a locally acting embryonic factor inducing trophinin expression by maternal cells (Figure 2, I to K). Thus trophinin expression by tubal epithelial cells depends on the presence of an embryo. This is in sharp contrast to mouse trophinin, whose expression is induced by the ovarian hormone, estrogen, independent of the embryo.[16,17]

In this study, we showed that hCG induces the levels of trophinin transcripts in the fallopian tube (Table 3). This must lead to an elevation of trophinin protein, which was detected by immunohistochemistry (Figure 4). In preimplantation stage human embryos, hCG-β transcripts are detected as early as the two-cell stage,[21] and preimplantation stage blastocysts secrete hCG.[22–24] Thus, it is likely that a human blastocyst secretes hCG before and during implantation. Given that trophinin mediates cell adhesion by homophilic binding,[11] evidence collectively suggests that hCG-β secreted from a blastocyst induces trophinin expression by the maternal epithelium, resulting in trophinin-mediated homophilic binding between the embryo and maternal epithelium.

Using fallopian tubal explants, we found that high concentrations (100 IU/ml) of hCG induce trophinin expression in epithelial cells (Figure 4, Table 3). This concentration of hCG has physiological relevance if local concentrations of hCG are considered. In pregnant women 6 to 12 days after ovulation the first sign of pregnancy is an hCG concentration of greater than 0.325 mIU/ml in the urine on the day of blastocyst implantation.[25] Urine from non-pregnant women shows no detectable levels of hCG, indicating that elevated hCG in urine is derived from an implanting blastocyst. As the concentration of hCG in the urine and plasma is similar and the plasma volume of a 50-kg woman is 1900 ml,[26] the total

Table 3. Quantitative Analysis of Trophinin mRNA in Explants of the Intact Fallopian Tube Incubated with hCG

	Incubation for 6 hours			Incubation for 24 hours		
	0*	10	100	0	10	100
Experiment 1†	15.8‡	35.4	431.2	1.1	31.2	38.7
Experiment 2	2.3	4.1	7.5	3.4	9.8	27.6

*, Concentration of hCG (IU/ml).
†, Experiments 1 and 2 were conducted using fallopian tubal explants obtained from each different individual who underwent hysterectomy.
‡, Trophinin:GAPDH mRNA ratios multiplied by 100 are indicated.

amount of hCG produced by the blastocyst is calculated to be 617.5 mIU (= 0.325 mIU/ml × 1900 ml). Estimating that local volume surrounding the blastcyst in the fallopian tube ranges from 1 μl to 10 μl, the intraluminal concentration of hCG around the blastocyst is estimated to be 617.5 ~ 61.8 IU/ml. Thus the maternal epithelia adjacent to an implanting embryo is likely to be exposed to high concentrations of hCG.

The timing and quantity of hCG produced by the embryo are considered key factors in determining whether a human pregnancy succeeds or fails.[27] Statistics of assisted reproduction show that the rate of gestation increases substantially when several embryos of the two-to-eight-cell stage are transferred into the uterus.[28] The experience of assisted reproduction also suggests that the quality of the oocyte largely determines the success of implantation.[29] In light of present findings, oocyte quality may be closely related to the activity of hCG secretion.

It is well known that tubal pregnancy frequently occurs in chronic salpingitis or salpingitis isthmica nodosa.[30] Since these conditions are associated with inflammation, it is likely that inflammatory destruction of the fallopian tube delays migration of blastocyst within the fallopian tube, thus causing the elevation of intraluminal concentrations of hCG. Such delays will also allow time for the blastocyst to interact with tubal epithelial cells. It is also possible that signal transduction through the luteinizing hormone receptor triggered by hCG binding is coupled to downstream signal transduction of inflammatory cytokines.[31,32] Thus cells undergoing inflammation may be more susceptible to stimulation by hCG.

Evidence suggests that there is cross-talk between the mouse blastocyst and uterus to ensure successful implantation.[33] Thus spaciotemporal actions of steroid hormones, various growth factors, and cytokines are thought to play important roles to prepare the receptive uterus for implantation. However, cellular interactions culminating in implantation and placentation vary significantly among mammalian species.[34,35] We found significant differences in the expression pattern and *in vivo* function of human and mouse trophinins.[16,17] Trophinin is strongly expressed in trophoblasts in the human placenta during early stage of pregnancy.[15] By contrast, trophinin is not expressed in trophoblastic cells during and after implantation in the mouse.[16] Lack of trophinin has no obvious effect on mouse blastocyst implantation.[17]

Genes encoding CG-β are found only in primates.[36,37] Nucleotide sequences of CG-β genes show significant diversion among primate species, and human CG-β diverged further from those found in non-human primates.[37–39] Considering these characteristics of human CG-β and the present findings of the activity of hCG on human trophinin gene expression (Table 3), it is likely that trophinin function in embryo implantation is unique to humans. If this is the case, then the activity of hCG on trophinin gene expression may form the basis of ectopic pregnancy, a condition unique to humans. Recently, possible involvement of hCG in tubal pregnancy was suggested based on the finding of hCG expression by the decidualized endometrium.[40] Further studies are needed to determine the role of hCG on the pathogeneisis of tubal pregnancy. Nonetheless, information obtained by studies on trophinin and CG-β will provide us with a clue for early detection and prevention of ectopic pregnancy.

Acknowledgments

We thank Dr. Koji Yoshinaga, National Institute of Child Health and Human Development, National Institutes of Health, for his helpful suggestions and discussions, and Ms. Akiko Ishida, Department of Pathology, Shinshu University School of Medicine, for her technical assistance.

References

1. Ectopic pregnancy—United States, 1990–1992. MMWR Morb Mortal Wkly Rep 1995, 44:46–48
2. Brenner PF, Roy S, Mishell Jr DR: Ectopic pregnancy: a study of 300 consecutive surgically treated cases. JAMA 1980, 243:673–676
3. Orsini MW, McLaren A: Loss of the zona pellucida in mice, and the effect of tubal ligation and ovariectomy. J Reprod Fertil 1967, 13:485–499
4. Tutton DA, Carr DH: The fate of trophoblast retained within the oviduct in the mouse. Gynecol Obstet Invest 1984, 17:18–24
5. Pauerstein CJ, Eddy CA, Koong MK, Moore GD: Rabbit endosalpinx suppresses ectopic implantation. Fertil Steril 1990, 54:522–526
6. Croxatto HB, Ortiz ME, Diaz S, Hess R, Balmaceda J, Croxatto HD: Studies on the duration of egg transport by the human oviduct: II. ovum location at various intervals following luteinizing hormone peak. Am J Obstet Gynecol 1978, 132:629–634
7. Aplin JD: The cell biological basis of human implantation. Baillieres Clin Obstet Gynaecol 2000, 14:757–764
8. Lessey BA: Endometrial receptivity and the window of implantation. Baillieres Clin Obstet Gynaecol 2000, 14:775–788
9. Kliman HJ, Coutifaris C, Babalola GO, Soto EA, Kao L-C, Queenan Jr JT, Feinberg RF, Strauss III JF: The human trophoblast: homotypic and heterotypic cell-cell interactions. Progress in Clinical and Biological Research 294: Development of Preimplantation Embryos and Their Environment. Edited by Yoshinaga K, Mori T. New York, Alan R Liss, 1989, pp 425–434
10. Sulz L, Valenzuela JP, Salvatierra AM, Ortiz ME, Croxatto HB: The expression of α_v and β_3 integrin subunits in the normal human fallopian tube epithelium suggests the occurrence of a tubal implantation window. Hum Reprod 1998, 13:2916–2920
11. Fukuda MN, Sato T, Nakayama J, Klier G, Mikami M, Aoki D, Nozawa S: Trophinin and tastin, a novel cell adhesion molecule complex with potential involvement in embryo implantation. Genes Dev 1995, 9:1199–1210
12. Suzuki N, Zara J, Sato T, Ong E, Bakhiet N, Oshima RG, Watson KL, Fukuda MN: A cytoplasmic protein, bystin, interacts with trophinin, tastin, and cytokeratin and may be involved in trophinin-mediated cell adhesion between trophoblast and endometrial epithelial cells. Proc Natl Acad Sci USA 1998, 95:5027–5032
13. Fukuda MN, Nozawa S: Trophinin, tastin, and bystin: a complex mediating unique attachment between trophoblastic and endometrial epithelial cells at their respective apical cell membranes. Semin Reprod Endocrinol 1999, 17:229–234
14. Fukuda MN, Nadano D, Suzuki N, Nakayama J: Potential involvement of trophinin, bystin, and tastin in embryo implantation. Embryo Implantation: Molecular, Cellular, and Clinical Aspects. Edited by Carson DD. New York, Springer-Verlag, 1999, pp 132–140
15. Suzuki N, Nakayama J, Shih IM, Aoki D, Nozawa S, Fukuda MN: Expression of trophinin, tastin, and bystin by trophoblast and endometrial cells in human placenta. Biol Reprod 1999, 60:621–627
16. Suzuki N, Nadano D, Paria BC, Kupriyanov S, Sugihara K, Fukuda MN: Trophinin expression in the mouse uterus coincides with implantation and is hormonally regulated but not induced by implanting blastocysts. Endocrinology 2000, 141:4247–4254
17. Nadano D, Sugihara K, Paria BC, Saburi S, Copeland NG, Gilbert DJ, Jenkins NA, Nakayama J, Fukuda MN: Significant differences be-

tween mouse and human trophinins are revealed by their expression patterns and targeted disruption of mouse trophinin gene. Biol Reprod 2002, 66:313–321
18. Ishihara K, Kurihara M, Goso Y, Urata T, Ota H, Katsuyama T, Hotta K: Peripheral α-linked N-acetylglucosamine on the carbohydrate moiety of mucin derived from mammalian gastric gland mucous cells: epitope recognized by a newly characterized monoclonal antibody. Biochem J 1996, 318:409–416
19. Kawakami M, Nakayama J: Enhanced expression of prostate-specific membrane antigen gene in prostate cancer as revealed by in situ hybridization. Cancer Res 1997, 57:2321–2324
20. Shimizu F, Nakayama J, Ishizone S, Zhang MX, Kawakubo M, Ota H, Sugiyama A, Kawasaki S, Fukuda M, Katsuyama T: Usefulness of the real-time reverse transcription-polymerase chain reaction assay targeted to α1,4-N-acetylglucosaminyltransferase for the detection of gastric cancer. Lab Invest 2003, 83:187–197
21. Jurisicova A, Antenos M, Kapasi K, Meriano J, Casper RF: Variability in the expression of trophectodermal markers β-human chorionic gonadotrophin, human leukocyte antigen-G, and pregnancy-specific β-1 glycoprotein by the human blastocyst. Hum Reprod 1999, 14: 1852–1858
22. Dokras A, Sargent IL, Gardner RL, Barlow DH: Human trophectoderm biopsy and secretion of chorionic gonadotrophin. Hum Reprod 1991, 6:1453–1459
23. Dimitriadou F, Phocas I, Mantzavinos T, Sarandakou A, Rizos D, Zourlas PA: Discordant secretion of pregnancy-specific β1-glycoprotein and human chorionic gonadotropin by human pre-embryos cultured in vitro. Fertil Steril 1992, 57:631–636
24. Lopata A, Oliva K, Stanton PG, Robertson DM: Analysis of chorionic gonadotrophin secreted by cultured human blastocysts. Mol Hum Reprod 1997, 3:517–521
25. Wilcox AJ, Baird DD, Weinberg CR: Time of implantation of the conceptus and loss of pregnancy. N Engl J Med 1999, 340:1796–1799
26. Wintrobe MM: Calculations and determination of red cell, plasma, and total blood volumes in adult men and women. Clinical Hematology. London, Lea & Febiger, 1974, pp 1792
27. Heam JP, Webley GE, Gildley-Baird AA: Chorionic gonadotropin and embryo-maternal recognition during peri-implantation period in primates. Reprod Fertil 1991, 92:497–507
28. Norwitz ER, Schust DJ, Fisher SJ: Implantation and the survival of early pregnancy. N Engl J Med 2001, 345:1400–1408
29. Sauer MV, Paulson RJ, Lobo RA: Reversing the natural decline in human fertility: an extended clinical trial of oocyte donation to women of advanced reproductive age. JAMA 1992, 268:1275–1279
30. Green LK, Kott ML: Histopathologic findings in ectopic tubal pregnancy. Int J Gynecol Pathol 1989, 8:255–262
31. Dufau ML: The luteinizing hormone receptor. Annu Rev Physiol 1998, 60:461–496
32. McFarland KC, Sprengel R, Phillips HS, Kohler M, Rosemblit N, Nikolics K, Segaloff DL, Seeburg PH: Lutropin-choriogonadotropin receptor: an unusual member of the G protein-coupled receptor family. Science 1989, 245:494–499
33. Paria BC, Reese J, Das SK, Dey SK: Deciphering the cross-talk of implantation: advances and challenges. Science 2002, 296:2185–2188
34. Carson DD, Bagchi I, Dey SK, Enders AC, Fazleabas AT, Lessey BA, Yoshinaga K: Embryo implantation. Dev Biol 2000, 223:217–237
35. Enders AC, Lantz KC, Peterson PE, Hendrickx AG: From blastocyst to placenta: the morphology of implantation in the baboon. Hum Reprod 1997, 3:561–573
36. Pierce JG, Parsons TF: Glycoprotein hormones: structure and function. Annu Rev Biochem 1981, 50:465–495
37. Maston GA, Ruvolo M: Chorionic gonadotropin has a recent origin within primates and an evolutionary history of selection. Mol Biol Evol 2002, 19:320–335
38. Talmadge K, Vamvakopoulos NC, Fiddes JC: Evolution of the genes for the β subunits of human chorionic gonadotropin and luteinizing hormone. Nature 1984, 307:37–40
39. Fiddes JC, Goodman HM: The cDNA for the β-subunit of human chorionic gonadotropin suggests evolution of a gene by readthrough into the 3′-untranslated region. Nature 1980, 286:684–687
40. Zimmermann G, Baier D, Majer J, Alexander H: Expression of beta hCG and alpha CG mRNA and hCG hormone in human decidual tissue in patients during tubal pregnancy. Mol Hum Reprod 2003, 9:81–89

Volume 51(12): 1689–1698, 2003
The Journal of Histochemistry & Cytochemistry
http://www.jhc.org

ARTICLE

Expression of Gastric Gland Mucous Cell-Type Mucin in Normal and Neoplastic Human Tissues

Kosei Nakajima, Hiroyoshi Ota, Mu Xia Zhang, Kenji Sano, Takayuki Honda, Keiko Ishii, and Jun Nakayama

Institute of Organ Transplants, Reconstructive Medicine and Tissue Engineering, Shinshu University Graduate School of Medicine (KN); Department of Biomedical Laboratory Sciences, School of Health Sciences, School of Medicine, Shinshu University (HO); Department of Laboratory Medicine, School of Medicine, Shinshu University (HO, MXZ,KS,TH,KI,JN); and Department of Pathology, School of Medicine, Shinshu University (JN), Matsumoto, Japan

SUMMARY Gastric gland mucous cells produce class III mucin, which is also found in Brunner's glands and mucous glands along the pancreaticobiliary tract, and in metaplasia and adenocarcinomas differentiating towards gastric mucosa. Recently, we showed that class III mucin possesses GlcNAcα1→4Galβ→R, formed by α1,4-*N*-acetylglucosaminyltransferase (α4GnT). Examining the tissue-specific expression of mucin epitopes is useful to clarify cell-lineage differentiation and to identify the site of origin of metastatic carcinomas in histological specimens. Formalin-fixed, paraffin-embedded tissue sections from esophagus, stomach, colon, liver, pancreas, lung, kidney, prostate, breast, and salivary gland resected for carcinoma, as well as salivary gland adenoma, colon adenoma, and metastatic adenocarcinoma of lymph nodes from stomach, pancreas, colon, and breast, were immunostained for MUC6, α4GnT, and GlcNAcα1→4Galβ→R. These were all expressed in normal, metaplastic, and adenocarcinoma tissues of stomach, pancreas, and bile duct, and in pulmonary mucinous bronchioloalveolar carcinomas. Cells expressing α4GnT uniformly expressed GlcNAcα1→4Galβ→R. Only MUC6 was expressed in normal salivary glands, pancreas, seminal vesicles, renal tubules, and colon adenomas, and in normal tissue and adenocarcinomas of prostate and breast. No tissues showed immunoreactivity for α4GnT alone. Immunohistochemistry (IHC) profiles were similar for metastatic carcinomas and primary carcinoma tissues. The IHC profiles for MUC6, α4GnT, and GlcNAcα1→4Galβ→R may be diagnostically relevant. (J Histochem Cytochem 51:1689–1698, 2003)

KEY WORDS
glycosyltransferase
gastric mucin
immunohistochemistry
mucin core protein

In GASTRIC MUCOSA, two types of mucus-secreting cells exist: the surface mucous cell and the gland mucous cell. The latter, which includes cardiac gland cells, mucous neck cells, and pyloric gland cells, possess class III mucin, as identified by paradoxical concanavalin A staining (Katsuyama and Spicer 1978; Suganuma et al. 1981; Ota et al. 2001). In normal human tissues, class III mucin is expressed in gastric gland mucous cells, Brunner's gland cells, and mucous cells of the accessory glands of the pancreaticobiliary tract (Katsuyama and Spicer 1978; Suganuma et al. 1981; Ota et al. 1991,1998; Nakamura et al. 1998). Class III mucin is also expressed in gastric metaplasia of the gallbladder (Tsutsumi et al. 1984) and mucinous metaplasia of the pancreas (Matsuzawa et al. 1992; Ota et al. 2001; Zhang et al. 2001), and in carcinoma of stomach (Akamatsu and Katsuyama 1990; Lesuffleur et al. 1994; Fujimori et al. 1995; Nakamura et al. 1998; Ota et al. 2001), bile duct (Kijima et al. 1989; Ota et al. 1995), gallbladder (Tsutsumi et al. 1984), and pancreas (Matsuzawa et al. 1992; Nakamura et al. 1998; Ota et al. 2001), as well as in mucinous bronchioloalveolar cell carcinoma of the lung (Honda et al. 1998; Ota et al. 2001) and adenoma malignum of the uterine cervix (Ishii et al. 1998,1999)

Correspondence to: Hiroyoshi Ota, Dept. of Biomedical Laboratory Sciences, School of Health Sciences, School of Medicine, Shinshu University, Matsumoto, Nagano 390-8621, Japan. E-mail: hohta@gipac.shinshu-u.ac.jp

Received for publication September 23, 2002; accepted July 18, 2003 (2A5923).

0022-1554/03/$3.30

Several years ago, Ishihara et al. (1996) raised a specific monoclonal antibody (MAb) against gastric mucin, designated HIK1083, which recognizes *N*-acetylglucosaminα1→4galactoseβ→R (GlcNAcα1→4Galβ→R). We found that the distribution of GlcNAcα1→4Galβ→R is consistent with the distribution of class III mucin in normal vertebrate tissues and in metaplastic and neoplastic human tissues (Nakamura et al. 1998; Ota et al. 1998,2001). More recently, we showed that class III mucin possesses this particular glycan, GlcNAcα1→4Galβ→R, which is formed by α1,4-*N*-acetylglucosaminyltransferase (α4GnT) (Nakayama et al. 1999), and that two distinct mucin core proteins, MUC5AC and MUC6, present in gastric mucin carry GlcNAcα1→4Galβ→R (Zhang et al. 2001).

Examining tissue-specific expression of mucin epitopes in human tissues is a useful way to clarify the cell-lineage differentiation of carcinoma cells and to demonstrate the site of origin of metastatic carcinomas in histological specimens.

GlcNAcα1→4Galβ→R is preferentially attached to core2-branched O-glycan (Ishihara et al. 1996). The sialyl Lewis X found in O-glycan are also attached to the terminal end of core2-branched structures (Fukuda 1996). Therefore, it appears that the expressions of GlcNAcα1→4Galβ→R and sialyl Lewis X may be

Table 1 Immunohistochemical expressions of MUC6, a4GnT, and GlcNAc α1→4Galβ→R in non-neoplastic tissues[a]

Tissue	*n*	MUC6	α4GnT	GlcNAc α1–4Galβ–R
Salivary gland	10			
Duct cells		0	0	0
Serous cells		0	0	0
Mucous cells		10/0.0 (0.0–0.0)[b]	0	0
Esophagus	10			
Squamous cells		0	0	0
Esophageal glands		0	0	0
Stomach	10			
Surface mucous cells		0	0	0
Gland mucous cells		100/3.0 (2.0–3.0)	100/1.0 (1.0–2.0)	100/3.0 (3.0–3.0)
Chief cells		0	0	0
Parietal cells		0	0	0
Duodenum	5			
Absorptive cells		0	0	0
Goblet cells		0	0	0
Brunner's glands		100/2.0 (1.0–2.0)	100/1.0 (1.0–1.25)	100/3.0 (3.0–3.0)
Colon	10			
Absorptive cells		0	0	0
Goblet cells		0	0	0
Pancreas				
Duct cells	10	30/0.0 (0.0–1.0)	20/0.0 (0.0–0.0)	30/0.0 (0.0–1.0)
Acinar cells	9	67/1.0 (0.0–1.0)	0	0
Centroacinar cells	9	67/1.0 (0.0–1.0)	0	0
Periductal cells	8	50/0.5 (0.0–1.0)	38/0.0 (0.0–1.0)	50/0.5 (0.0–1.0)
Mucinous metaplasia	7	100/1.0 (1.0–1.0)	86/1.0 (1.0–1.0)	100/1.0 (1.0–1.0)
Liver				
Intrahepatic bile duct	9	100/1.0 (1.0–1.25)	89/1.0 (1.0–1.0)	100/1.0 (1.0–1.0)
Periductal glands	4	100/2.0 (1.5–2.0)	100/2.0 (1.5–2.0)	100/1.5 (1.0–2.0)
Hepatocytes	10	0	0	0
Lung	10			
Alveolar cells		0	0	0
Bronchial epithelial cells		0	0	0
Accessory glands		0	0	0
Kidney				
Glomerulus	10	0	0	0
Tubule cells	10	100/1.0 (1.0–1.0)	0	0
Transitional cells	6	0	0	0
Prostate gland	10	30/0.0 (0.0–1.0)	0	0
Seminal vesicle	7	100/2.0 (1.25–2.0)	0	0
Mammary gland	8			
Duct cells		0	0	0
Lobular cells		50/0.5 (0.0–1.0)	0	0

[a]Scores are expressed as positive rate %/median score (25 percentile–75 percentile).
[b]Positive rate %/median score (25 percentile–75 percentile).

reciprocally regulated, because these carbohydrates compete for the common precursor oligosaccharide, core2-branched O-glycan. It is well known that sialyl Lewis X serve as preferential ligands for the cell-adhesion molecules E- and P-selectin (Fukushima et al. 1984; Itzkowitz et al. 1988; Rosen and Bertozzi 1994). Recently we demonstrated that, in colorectal and pulmonary cancers, the sialyl Lewis X expressed on core2-branched O-glycans showed a positive correlation with tumor progression (Shimodaira et al. 1997; Machida et al. 2001).

We designed the present study to explore the IHC expressions of MUC6, α4GnT, and GlcNAcα1→4Galβ→R in human normal, metaplastic, and adenocarcinoma tissues. We also examined the IHC expressions of GlcNAcα1→4Galβ→R and sialyl Lewis X in gastric carcinomas and in metastatic gastric carcinomas of lymph nodes.

Materials and Methods

Preparation of Tissues

Formalin-fixed, paraffin-embedded sections of human tissues were obtained from the surgical pathology files of the Department of Clinical Laboratory, Shinshu University Hospital, Matsumoto, Japan. Specimens consisted of histologically normal portions of tissues resected for adenoma or carcinoma and various tumor tissues, as well as metastatic adenocarcinomas of lymph nodes from stomach, colon, pancreas, and breast (Tables 1 and 2). This study was performed after written informed consent had been obtained from the patients.

Histochemistry

Serial paraffin sections of 3-μm thickness were stained with H&E for histological examination or immunostained with anti-MUC6 (Novocastra; Newcastle-upon-Tyne, UK), anti-α4GnT (Zhang et al. 2001), or GlcNAcα1→4Galβ→R (MAb

Table 2 Immunohistochemical expression of MUC6, α4GnT, GlcNAc α1-4Gal β-R, and sialyl Lewis X in neoplastic tissues at primary and metastatic lesions[a]

Tissue	*n*	MUC6	α4GnT	GlcNAc α1-4Gal β-R	Sialyl Lewis X
Stomach					
Diffuse type adenocarcinoma					
Early	9	78/1.0 (0.75–1.25)	67/1.0 (0.0–1.0)	89/2.0 (1.0–2.0)	56/1.0 (0.0–1.0)
Advanced	14	57/1.0 (0.0–1.0)	50/0.5 (0.0–1.0)	64/1.0 (0.0–1.0)	71/1.0 (0.0–2.0)
Total	23	65/1.0 (0.0–1.0)	57/1.0 (0.0–1.0)	74/1.0 (0.25–2.0)	65/1.0 (0.0–1.75)
Intestinal type adenocarcinoma					
Early	11	82/1.0 (1.0–1.0)	64/1.0 (0.0–1.0)	73/1.0 (0.25–1.0)	100/1.0 (1.0-2.0)
Advanced	6	83/1.5 (1.0–2.0)	50/0.5 (0.0-1.0)	50/0.5 (0.0–1.0)	83/1.0 (1.0-1.0)
Total	17	82/1.0 (1.0–1.25)	59/1.0 (0.0–1.0)	65/1.0 (0.0–1.0)	94/1.0 (1.0–2.0)
Lymph node metastasis	9	78/1.0 (0.75–1.0)	56/1.0 (0.0–1.0)	67/2.0 (0.0–2.0)	56/1.0 (0.0–3.0)
Pancreas					
Adenocarcinoma	14	71/1.0 (0.0–1.0)	71/1.0 (0.0–1.0)	86/1.0 (1.0–1.0)	NE
Lymph node metastasis	4	75/1.0 (0.5–1.0)	50/0.5 (0.0–1.0)	75/1.0 (0.5–1.5)	NE
Liver					
Cholangiocellular carcinoma	10	90/1.0 (1.0–1.0)	60/1.0 (0.0–1.0)	60/1.0 (0.0–1.0)	NE
Hepatocellular carcinoma	10	0	0	0	NE
Lung					
Mucinous BAC	4	100/1.5 (1.0–2.0)	100/1.0 (1.0–1.0)	100/1.0 (1.0–1.0)	NE
Other type adenocarcinoma	20	0	0	0	NE
Colon					
Adenoma	53	2/0.0 (0.0–0.0)	0	0	NE
Adenocarcinoma	22	0	0	0	NE
Lymph node metastasis	7	0	0	0	NE
Prostate gland					
Adenocarcinoma	9	33/0.0 (0.0–1.0)	0	0	NE
Mammary gland					
Mucinous carcinoma	10	50/0.5 (0.0–1.0)	0	0	NE
Lobular carcinoma	10	40/0.0 (0.0–1.0)	0	0	NE
Other type carcinoma	10	60/1.0 (0.0–1.0)	0	0	NE
Lymph node metastasis	5	60/1.0 (0.0–1.0)	0	0	NE
Salivary gland					
Adenoid cystic carcinoma	5	0	0	0	NE
Kidney					
Renal cell carcinoma	8	0	0	0	NE

[a]Scores are expressed as positive rate %/median score (25 percentile–75 percentile). NE, not examined.

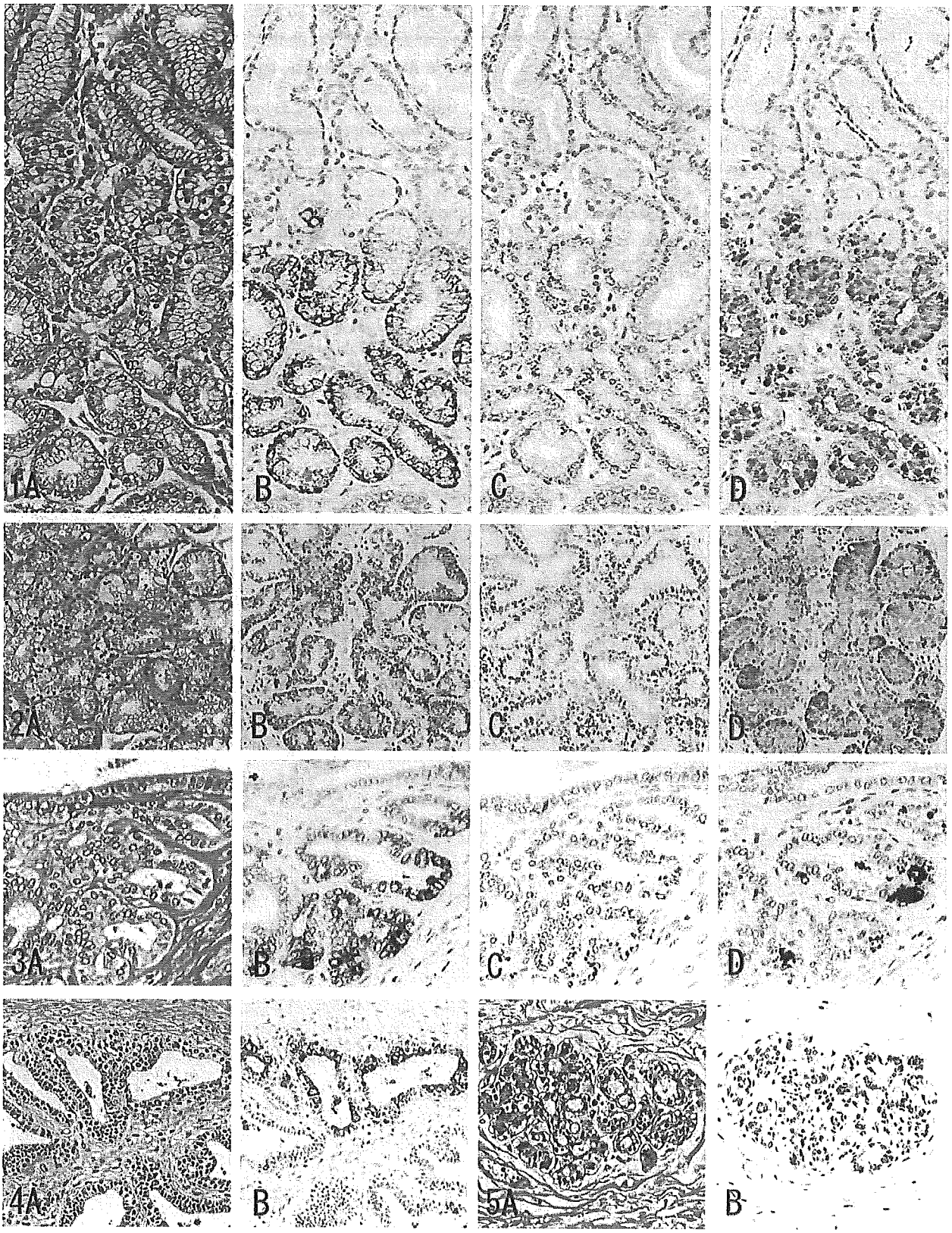
1A
B
C
D
2A
B
C
D
3A
B
C
D
4A
B
5A
B

HIK1083; Kanto Chemical, Tokyo, Japan). To facilitate comparison of the distributions of antigens, mirror paraffin sections of 3-μm thickness from gastric adenocarcinomas and metastatic adenocarcinomas of lymph nodes from gastric adenocarcinomas expressing both GlcNAcα1→4Galβ→R and sialyl Lewis X in primary sites were stained with HIK1083 or NCC-ST439 MAb (Kumamoto et al. 1998) (Nippon Kayaku; Tokyo, Japan) specific for the sialyl Lewis X attached to O-glycan.

IHC staining was performed using the Envision+ method (DAKO; Carpinteria, CA). Briefly, sections were dewaxed and rehydrated and endogenous peroxidase activity was blocked with 0.3% H_2O_2 in methanol (30 min). Before immunostaining, antigen retrieval was carried out using a microwave (600 W) for 25 min in 0.01 mol/liter citrate buffer (pH 6.0) for both GlcNAcα1→4Galβ→R and MUC6. For immunostaining with anti-α4GnT and sialyl Lewis X, antigen retrieval was not carried out. The tissue sections were blocked with 5% normal bovine serum albumin in Tris-buffered saline (TBS; 140 mmol/liter NaCl, 50 mmol/liter Tris-HCl, pH 7.6) and incubated with primary antibodies. After washing in TBS, slides were incubated with peroxidase and second antibody-labeled polymer (DAKO) for 60 min. The reaction was developed with 3,3′-diaminobenzidine (Sigma Chemical; Poole, UK) containig 0.02% H_2O_2. For immunostaining of seminal vesicles, the Envision+ method for immunoalkaline phosphatase (DAKO) was used. Sections were lightly counterstained with hematoxylin, dehydrated, cleared in xylene, and mounted in synthetic medium.

Negative controls were obtained by omitting the primary antibody. The gastric gland mucous cells and Brunner's gland cells in the specimens were used as internal positive controls for MUC6, anti-α4GnT, and GlcNAcα1→4Galβ→R. Colon adenocarcinoma tissues were used as positive controls for sialyl Lewis X.

Evaluation of Immunostaining

The degree of staining in tissues examined with specific antibodies was scored semiquantitatively as 0 (negative), 1 (less than one third of the tissue), 2 (more than one third but less than two thirds), or 3 (more than two thirds). Grading of immunoreactivity was carried out by a single observer (KN). To validate the grading method, all specimens were graded twice, on two separate occasions. There was no significant intraobserver variation.

Statistics

The Mann–Whitney *U*-test was used to compare the scores given for immunoreactivities. Spearman's correlation coefficient by rank was used to analyze the correlations among the immunoreactivity scores given for MUC6, α4GnT, GlcNAcα1→4Galβ→R, and sialyl Lewis X. Staining scores are nonparametric and are presented as median rather than mean values.

Results

Demonstration of MUC6, α4GnT, and GlcNAcα1→4Galβ→R in Non-neoplastic Tissues

MUC6 was diffusely expressed in the cytoplasm (Figures 1B, 2B, 3B, 4B, and 5B), while α4GnT was expressed in the Golgi area (Figures 1C, 2C, and 3C). GlcNAcα1→4Galβ→R was mainly localized in cytoplasmic mucus granules (Figures 1D, 2D, and 3D), although in some cells it was localized on the apical cytoplasmic membrane.

MUC6, α4GnT, and GlcNAcα1→4Galβ→R were present in discrete cell types to various degrees: gastric gland mucous cells (Figure 1) (cardiac gland cells, mucous neck cells, and pyloric gland cells), Brunner's gland cells (Figure 2), mucous cells of the periductal glands of the pancreaticobiliary tracts (Figure 3), biliary tract epithelial cells, and mucous cells of mucinous metaplasia of the pancreatic ducts. In these tissues, α4GnT-positive cells always exhibited immunoreactivity for GlcNAcα1→4Galβ→R, as described previously (Zhang et al. 2001).

Figures 1–5

Figure 1 (A–D) IHC staining for MUC6, α4GnT, and GlcNAcα1→4Galβ→R in normal pyloric mucosa, prepared from serial sections. In pyloric glands (A), MUC6 is diffusely expressed in the cytoplasm (B), α4GnT is expressed in the Golgi area (C), and GlcNAcα1→4Galβ→R is expressed in cytoplasmic mucus granules (D). H&E staining (A) and immunostaining for MUC6 (B), α4GnT (C), and GlcNAcα1→4Galβ→R (D). Original magnification ×200.

Figure 2 (A–D) IHC staining for MUC6, α4GnT, and GlcNAcα1→4Galβ→R in Brunner's glands, prepared from serial sections. In Brunner's glands (A), MUC6 is diffusely expressed in the cytoplasm (B), α4GnT is expressed in the Golgi area (C), and GlcNAcα1→4Galβ→R is expressed in cytoplasmic mucus granules (D). H&E staining (A) and immunostaining for MUC6 (B), α4GnT (C), and GlcNAcα1→4Galβ→R (D). Original magnification ×200.

Figure 3 (A–D) IHC staining for MUC6, α4GnT, and GlcNAcα1→4Galβ→R in peribiliary glands, prepared from serial sections. In peribiliary glands (A), MUC6 is diffusely expressed in cytoplasm (B), α4GnT is expressed in the Golgi area (C), and GlcNAcα1→4Galβ→R is expressed in cytoplasmic mucous granules (D). H&E staining (A) and immunostaining for MUC6 (B), α4GnT (C), and GlcNAcα1→4Galβ→R (D). Original magnification ×400.

Figure 4 IHC staining for MUC6 in normal prostate gland, prepared from serial sections. Some prostate gland cells show diffuse cytoplasmic expression of MUC6. H&E staining (A) and immunostaining for MUC6 (B). Original magnification ×250.

Figure 5 IHC staining for MUC6 in normal mammary gland, prepared from serial sections. Some cells of the terminal duct lobular unit of mammary gland show diffuse cytoplasmic expression of MUC6. H&E staining (A) and immunostaining for MUC6 (B). Original magnification ×300.

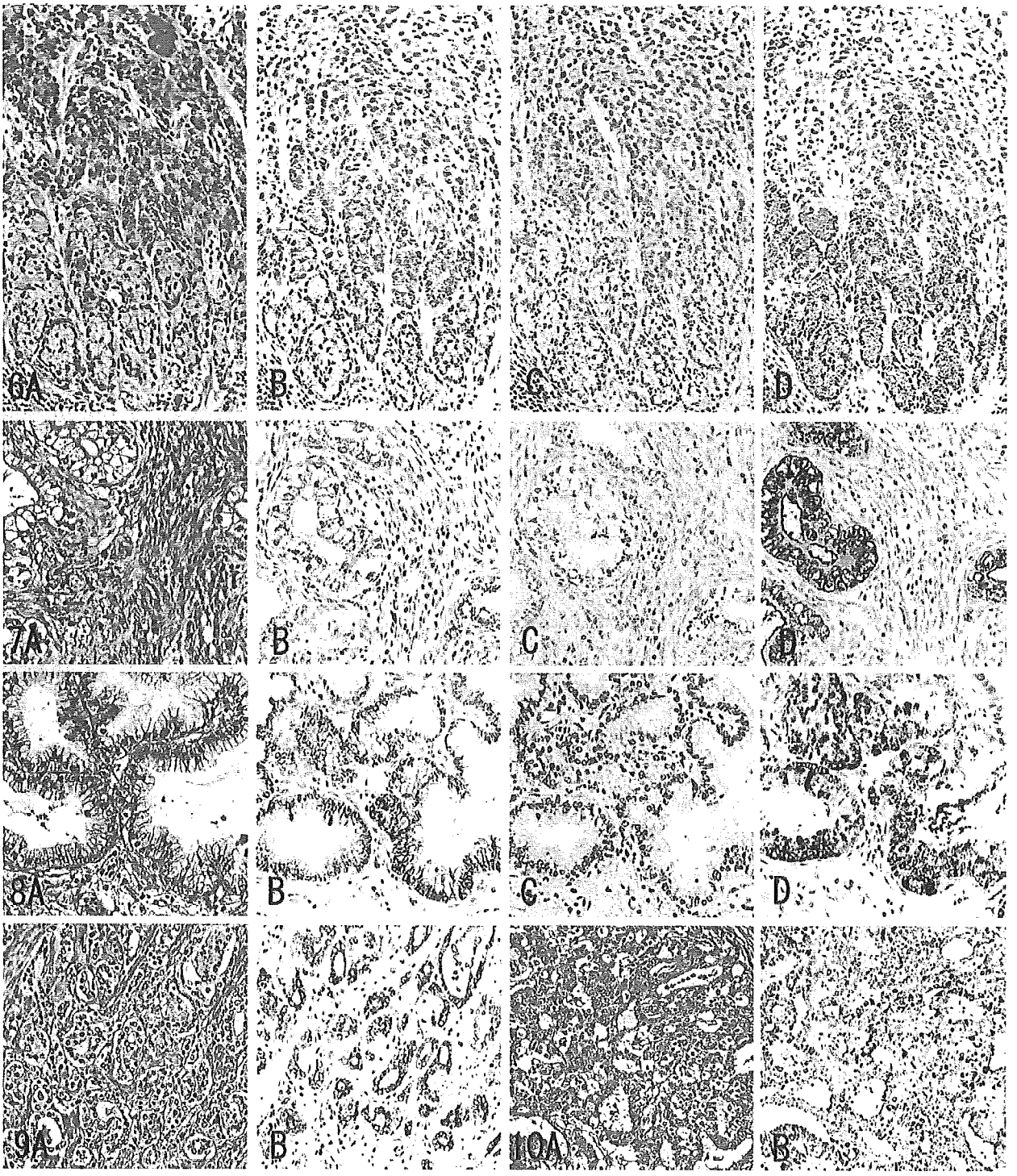

Figures 6–10

Figure 6 **(A–D)** IHC staining for MUC6, α4GnT, and GlcNAcα1→4Galβ→R in diffuse type gastric carcinoma, prepared from serial sections. In signet-ring carcinoma cells located in the lower portion **(A)**, MUC6 is diffusely expressed in the cytoplasm **(B)**, α4GnT is expressed in the Golgi area **(C)**, and GlcNAcα1→4Galβ→R is expressed in the cytoplasmic mucous granules **(D)**. H&E staining **(A)** and immunostaining for MUC6 **(B)**, α4GnT **(C)**, and GlcNAcα1→4Galβ→R **(D)**. Original magnification ×200.

Figure 7 **(A–D)** IHC staining for MUC6, α4GnT, and GlcNAcα1→4Galβ→R in pancreatic duct carcinoma, prepared from serial sections. In carcinoma cells **(A)**, MUC6 is diffusely expressed in the cytoplasm **(B)**, α4GnT is expressed in the Golgi area **(C)**, and GlcNAcα1→4Galβ→R is ex-

Except in the case of biliary tract epithelial cells, GlcNAcα1→4Galβ→R was found in cytoplasmic mucus granules. The biliary tract epithelial cells exhibited cytoplasmic and apical cytoplasmic membrane staining for GlcNAcα1→4Galβ→R.

MUC6 without α4GnT and GlcNAcα1→4Galβ→R was expressed in a minority of submandibular gland mucous cells, pancreatic centroacinar cells, renal tubules, prostate glands (Figure 4), and terminal duct lobular units of mammary glands (Figure 5), and was also strongly expressed in seminal vesicle epithelial cells.

MUC6, α4GnT, and GlcNAcα1→4Galβ→R were not detected in normal esophagus, colon, hepatocytes, or lungs. The IHC data presented here are summarized in Table 1.

Demonstration of MUC6, α4GnT, and GlcNAcα1→4Galβ→R in Neoplastic Tissues in Primary Tissues

MUC6, α4GnT, and GlcNAcα1→4Galβ→R were detected in carcinoma of the stomach (Figure 6), pancreas (Figure 7), and intrahepatic bile duct, and in mucinous bronchioloalveolar cell carcinoma (Figure 8). Staining differed quantitatively from case to case (Table 2).

In these tumor tissues, MUC6 exhibited a heterogeneous cytoplasmic expression (Figures 6B, 7B, 8B, 9B, and 10B), whereas α4GnT exhibited Golgi staining (Figures 6C, 7C, and 8C). GlcNAcα1→4Galβ→R was expressed on the luminal surface of anaplastic glands and in secreted mucins, as well as in the cytoplasm of carcinoma cells (Figures 6D, 7D, and 8D). In these tissues, α4GnT-positive cells uniformly exhibited GlcNAcα1→4Galβ→R.

In gastric carcinomas, the staining scores given for GlcNAcα1→4Galβ→R in diffuse-type carcinomas were greater in early carcinomas than in advanced carcinomas ($p<0.05$). The staining scores for α4GnT and MUC6 showed no relation to the depth of invasion of the carcinoma. No significant difference was found among the scores given for MUC6, α4GnT, and GlcNAcα1→4Galβ→R, irrespective of histological type or depth of wall penetration. The scores given for GlcNAcα1→4Galβ→R showed a significant correlation with those given for α4GnT ($r=0.73$ in diffuse-type gastric carcinomas; $r=0.86$ in intestinal-type carcinomas). There was no correlation between the scores for α4GnT and MUC6 or between those for MUC6 and GlcNAcα1→4Galβ→R.

In pancreatic carcinomas, there was no significant difference among the scores given for MUC6, α4GnT, and GlcNAcα1→4Galβ→R expression. The degree of GlcNAcα1→4Galβ→R expression showed a significant correlation with the degree of expression for α4GnT and for MUC6 ($r=0.65$ and $r=0.65$, respectively).

In cholangiocarcinomas, there was no significant difference among the staining scores for MUC6, α4GnT, and GlcNAcα1→4Galβ→R. The degree of GlcNAcα1→4Galβ→R expression showed a significant correlation with that of α4GnT expression ($r=0.91$). There was no correlation between MUC6 expression and α4GnT expression or between GlcNAcα1→4Galβ→R expression and MUC6 expression.

In mucinous bronchioloalveolar carcinomas, the scores given for GlcNAcα1→4Galβ→R were significantly higher than those for α4GnT expression ($p<0.05$). There were no correlations among the scores for MUC6, α4GnT, and GlcNAcα1→4Galβ→R.

In a minority of colon adenomas, prostate carcinomas (Figure 9), and breast carcinomas (Figure 10), MUC6 was detected, whereas α4GnT and GlcNAcα1→4Galβ→R were not. These IHC data are summarized in Table 2.

Demonstration of MUC6, α4GnT, and GlcNAcα1→4Galβ→R in Metastatic Adenocarcinomas of Lymph Nodes

Gastric carcinomas and pancreatic carcinomas showed immunoreactivity for MUC6, α4GnT, and GlcNAcα1→4Galβ→R. In gastric carcinomas, the degree of GlcNAcα1→4Galβ→R expression showed a signifi-

pressed in cytoplasmic mucous granules (D). H&E staining (A) and immunostaining for MUC6 (B), α4GnT (C), and GlcNAcα1→4Galβ→R (D). Original magnification ×250.

Figure 8 (A–D) IHC staining for MUC6, α4GnT, and GlcNAcα1→4Galβ→R in pulmonary mucinous bronchioloalveolar cell carcinoma, prepared from serial sections. In carcinoma cells (A), MUC6 is diffusely expressed in the cytoplasm (B), α4GnT is expressed in the Golgi area (C), and GlcNAcα1→4Galβ→R is expressed in cytoplasmic mucous granules (D). H&E staining (A) and immunostaining for MUC6 (B), α4GnT (C), and GlcNAcα1→4Galβ→R (D). Original magnification ×300.

Figure 9 IHC staining for MUC6 in prostatic adenocarcinoma, prepared from serial sections. Some carcinoma cells show diffuse cytoplasmic expression of MUC6. H&E staining (A) and immunostaining for MUC6 (B). Original magnification ×250.

Figure 10 IHC staining for MUC6 in breast carcinoma, prepared from serial sections. Some carcinoma cells show diffuse cytoplasmic expression of MUC6. H&E staining (A) and immunostaining for MUC6 (B). Original magnification ×200.

Figure 11 IHC staining for GlcNAcα1→4Galβ→R and sialyl Lewis X in gastric carcinoma, prepared from mirror sections. The distribution of the carcinoma cells reactive for GlcNAcα1→4Galβ→R was completely different from that of the carcinoma cells reactive for sialyl Lewis X. Immunostaining for GlcNAcα1→4Galβ→R (**A**) and sialyl Lewis X (**B**). Original magnification ×200.

cant correlation with the degree of α4GnT expression in gastric carcinomas (r=0.79). In both gastric carcinomas and pancreatic carcinomas, α4GnT-positive cells uniformly co-expressed GlcNAcα1→ 4Galβ→R. Breast carcinomas showed immunoreactivity only for MUC6. Colon carcinomas showed immunoreactivity for none of these antigens.

These IHC data are summarized in Table 2.

Demonstration of GlcNAcα1→4Galβ→R and Sialyl Lewis X in Gastric Carcinomas and Metastatic Gastric Carcinomas of Lymph Nodes

The distribution of carcinoma cells reactive for GlcNAcα1→4Galβ→R was completely different from that of carcinoma cells reactive for sialyl Lewis X both in primary (Figure 11) and in metastatic sites, although we found no negative correlation between GlcNAcα1→4Galβ→R and sialyl Lewis X expression. Carcinoma cells expressing both GlcNAcα1→ 4Galβ→R and sialyl Lewis X were not found.

These IHC data are summarized in Table 2.

Discussion

In this study we evaluated the IHC expressions of MUC6, α4GnT, and GlcNAcα1→4Galβ→R in normal, metaplastic, and neoplastic human tissues. The results showed (a) that α4GnT and GlcNAcα1→ 4Galβ→R were co-located in discrete cell-types (a finding consistent with involvement of α4GnT in the formation of GlcNAcα1→4Galβ→R in normal, metaplastic, and neoplastic cells) and (b) that both primary carcinoma tissues and metastatic tissues showed similar IHC profiles with regard to the expressions of MUC6, α4GnT, and GlcNAcα1→ 4Galβ→R.

In this study we have confirmed and extended our knowledge regarding the specific distribution of GlcNAcα1→4Galβ→R in human tissues. GlcNAcα1→ 4Galβ→R has been reported to be present in gastric gland mucous cells (cardiac gland cells, mucous neck

cells, and pyloric gland cells), Brunner's gland cells, mucous cells of the periductal glands of the pancreaticobiliary tract, mucinous metaplasia of gallbladder and pancreas, and neoplastic cells expressing gastric mucins [including mucinous tumors of the ovary, adenocarcinomas of stomach, pancreas, gallbladder, lung (mucinous bronchioloalveolar cell carcinoma), and uterine cervix (adenoma malignum) (Nakamura et al. 1998; Ota et al. 1998,2001; Zhang et al. 2001)], but not in normal esophagus, colon, pancreas, ovary, lung, uterine cervix, normal and neoplastic salivary glands, or adenocarcinomas of colon, breast, kidney, thyroid gland, endometrium, liver, or prostate (Ishii et al. 1998; Nakamura et al. 1998; Ota et al. 2001). In addition, we found that GlcNAcα1→4Galβ→R was present in the normal epithelium of the intrahepatic bile ducts and cholangiocarcinoma but not in seminal vesicle epithelium.

In this study, α4GnT-positive cells uniformly co-expressed GlcNAcα1→4Galβ→R, irrespective of whether the sections were from normal, metaplastic, or neoplastic tissues. The degree of GlcNAcα1→4Galβ→R expression showed a significant correlation with the degree of α4GnT expression in various adenocarcinoma tissues, as well as in normal and metaplastic cells.

The expressions of α4GnT and GlcNAcα1→4Galβ→R were more restricted than that of MUC6. MUC6 has been demonstrated to be present in human tissues in which both α4GnT and GlcNAcα1→4Galβ→R were positive, such as normal stomach (Ho et al. 1995a,b; Buisine et al. 2000b; Machado et al. 2000; Reis et al. 2000), duodenum (Bartman et al. 1998; Buisine et al. 2000a), bile duct (Bartman et al. 1998; Buisine et al. 2000a), gallbladder (Bartman et al. 1998; Buisine et al. 2000a), and in adenocarcinomas of the stomach (Ho et al. 1995b; Machado et al. 2000; Reis et al. 2000), bile duct (Bartman et al. 1998), gallbladder (Bartman et al. 1998; Sasaki et al. 1999), and pancreas (Bartman et al. 1998; Terada et al. 1996). As previously reported and confirmed in this study, MUC6 was distributed in a wide variety of human tissues in which both α4GnT and GlcNAcα1→4Galβ→R were negative. Thus, MUC6 has previously been demonstrated in normal endometrium (Bartman et al. 1998) and seminal vesicles (Bartman et al. 1998), adenoma of the colon (Bartman et al. 1999), and normal and adenocarcinoma of the breast (Bartman et al. 1998; Pereira et al. 2001).

The distribution of carcinoma cells reactive for GlcNAcα1→4Galβ→R was completely different from that of carcinoma cells reactive for sialyl Lewis X, both in primary (Figure 11) and metastatic sites, although we found no negative correlation between the GlcNAcα1→4Galβ→R and sialyl Lewis X expressions. GlcNAcα1→4Galβ→R is preferentially attached to core2-branched O-glycan (Ishihara et al. 1996), and the sialyl Lewis X found in O-glycan is also attached to the terminal end of core2-branched structures (Fukuda 1996). Therefore, the expressions of GlcNAcα1→ 4Galβ→R and sialyl Lewis X may be reciprocally regulated because these carbohydrates compete for the common precursor oligosaccharide, core2-branched O-glycan. It is well known that sialyl Lewis X serve as preferential ligands for the cell-adhesion molecules E- and P-selectin (Fukushima et al. 1984; Itzkowitz et al. 1988; Rosen and Bertozzi 1994). Recently, we demonstrated that the sialyl Lewis X expressed on core2-branched O-glycans were positively correlated with tumor progression in both colorectal and pulmonary cancers (Shimodaira et al. 1997; Machida et al. 2001). Overall, these results suggest that the expression of GlcNAcα1→4Galβ→R in gastric cancer cells may be a favorable predictor of the patient's outcome. Further study will be needed to test this hypothesis.

In summary, primary carcinoma tissues and metastatic tissues showed similar IHC profiles with regard to the expressions of MUC6, α4GnT, and GlcNAcα1→ 4Galβ→R. Determination of the site of origin of metastatic carcinomas using examination of histological slides continues to present a diagnostic challenge for the pathologist. It is possible that immunostaining for GlcNAcα1→4Galβ→R (with MAb HIK1083), or α4GnT, in conjunction with immunostaining for MUC6, could be diagnostically relevant because of their specific distributions in human tissues.

Acknowledgments

Supported by Grants-in-Aid for Scientific Research C-15590482 (to HO) and Priority Area 14082201 (to JN) from the Ministry of Education, Culture, Sports, Science and Technology of Japan.

We thank Professor Tsutomu Katsuyama and Katsunori Sasaki at Shinshu University School of Medicine, and Professor David Y. Graham at Baylor College of Medicine (Houston, TX) for their helpful comments and encouragement.

Literature Cited

Akamatsu T, Katsuyama T (1990) Histochemical demonstration of mucins in the intramucosal laminated structure of human gastric signet ring cell carcinoma and its relation to submucosal invasion. Histochem J 22:416–425

Bartman AE, Buisine MP, Aubert JP, Niehans GA, Toribara NW, Kim YS, Kelly EJ, et al. (1998) The MUC6 secretory mucin gene is expressed in a wide variety of epithelial tissues. J Pathol 186:398–405

Bartman AE, Sanderson SJ, Ewing SL, Niehans GA, Wiehr CL, Evans MK, Ho SB (1999) Aberrant expression of MUC5AC and MUC6 gastric mucin genes in colorectal polyps. Int J Cancer 80:210–218

Buisine MP, Devisme L, Degand P, Dieu MC, Gosselin B, Copin MC, Aubert JP, et al. (2000a) Developmental mucin gene expression in the gastroduodenal tract and accessory digestive glands. II. Duodenum and liver, gallbladder, and pancreas. J Histochem Cytochem 48:1667–1676

Buisine MP, Devisme L, Maunoury V, Deschodt E, Gosselin B, Copin MC, Aubert JP, et al. (2000b) Developmental mucin gene expression in the gastroduodenal tract and accessory digestive glands. I. Stomach. A relationship to gastric carcinoma. J Histochem Cytochem 48:1657–1666

Fujimori Y, Akamatsu T, Ota H, Katsuyama T (1995) Proliferative markers in gastric carcinoma and organoid differentiation. Hum Pathol 26:725–734

Fukuda M (1996) Possible roles of tumor-associated carbohydrate antigens. Cancer Res 56:2237–2244

Fukushima K, Hirota M, Terasaki PI, Wakisaka A, Togashi H, Chia D, Suyama N, et al. (1984) Characterization of sialosylated Lewis^x as a new tumor-associated antigen. Cancer Res 44:5279–5285

Ho SB, Roberton AM, Shekels LL, Lyftogt CT, Niehans GA, Toribara NW (1995a) Expression cloning of gastric mucin complementary DNA and localization of mucin gene expression. Gastroenterology 109:735–747

Ho SB, Shekels LL, Toribara NW, Kim YS, Lyftogt C, Cherwitz DL, Niehans GA (1995b) Mucin gene expression in normal, preneoplastic, and neoplastic human gastric epithelium. Cancer Res 55:2681–2690

Honda T, Ota H, Ishii K, Nakamura N, Kubo K, Katsuyama T (1998) Mucinous bronchioloalveolar carcinoma with organoid differentiation simulating the pyloric mucosa of the stomach: clinicopathologic, histochemical, and immunohistochemical analysis. Am J Clin Pathol 109:423–430

Ishihara K, Kurihara M, Goso Y, Urata T, Ota H, Katsuyama T, Hotta K (1996) Peripheral α-linked N-acetylglucosamine on the carbohydrate moiety of mucin derived from mammalian gastric gland mucous cells: epitope recognized by a newly characterized monoclonal antibody. Biochem J 318:409–416

Ishii K, Hosaka N, Toki T, Momose M, Hidaka E, Tsuchiya S, Katsuyama T (1998) A new view of the so-called adenoma malignum of the uterine cervix. Virchows Arch 432:315–322

Ishii K, Katsuyama T, Ota H, Watanabe T, Matsuyama I, Tsuchiya S, Shiozawa T, et al. (1999) Cytologic and cytochemical features of adenoma malignum of the uterine cervix. Cancer 87:245–253

Itzkowitz SH, Yuan M, Fukushi Y, Lee H, Shi ZR, Zurawski V Jr, Hakomori S, et al. (1988) Immunohistochemical comparison of Le^a, monosialosyl Le^a (CA 19–9), and disialosyl Le^a antigens in human colorectal and pancreatic tissues. Cancer Res 48:3834–3842

Katsuyama T, Spicer SS (1978) Histochemical differentiation of complex carbohydrates with variants of the concanavalin A–horseradish peroxidase method. J Histochem Cytochem 26: 233–250

Kijima H, Watanabe H, Iwafuchi M, Ishihara N (1989) Histogenesis of gallbladder carcinoma from investigation of early carcinoma and microcarcinoma. Acta Pathol Jpn 39:235–244

Kumamoto K, Mitsuoka C, Izawa M, Kimura N, Otsubo N, Ishida H, Kiso M, et al. (1998) Specific detection of sialyl Lewis X determinant carried on the mucin GlcNAcbeta1→6GalNAcalpha core structure as a tumor-associated antigen. Biochem Biophys Res Commun 247:514–517

Lesuffleur T, Zweibaum A, Real FX (1994) Mucins in normal and neoplastic human gastrointestinal tissues. Crit Rev Oncol Hematol 17:153–180

Machado JC, Nogueira AM, Carneiro F, Reis CA, Sobrinho-Simoes M (2000) Gastric carcinoma exhibits distinct types of cell differentiation: an immunohistochemical study of trefoil peptides (TFF1 and TFF2) and mucins (MUC1, MUC2, MUC5AC, and MUC6). J Pathol 190:437–443

Machida E, Nakayama J, Amano J, Fukuda M (2001) Clinicopathological significance of core 2 β1,6-N-acetylglucosaminyltransferase messenger RNA expressed in the pulmonary adenocarcinoma determined by in situ hybridization. Cancer Res 61:2226–2231

Matsuzawa K, Akamatsu T, Katsuyama T (1992) Mucin histochemistry of pancreatic duct cell carcinoma, with special reference to organoid differentiation simulating gastric pyloric mucosa. Hum Pathol 23:925–933

Nakamura N, Ota H, Katsuyama T, Akamatsu T, Ishihara K, Kurihara M, Hotta K (1998) Histochemical reactivity of normal, metaplastic, and neoplastic tissues to α-linked N-acetylglucosamine residue-specific monoclonal antibody HIK1083. J Histochem Cytochem 46:793–801

Nakayama J, Yeh JC, Misra AK, Ito S, Katsuyama T, Fukuda M (1999) Expression cloning of a human α1,4-N-acetylglucosaminyltransferase that forms GlcNAcα1→4Galβ→R, a glycan specifically expressed in the gastric gland mucous cell-type mucin. Proc Natl Acad Sci USA 96:8991–8996

Ota H, Hayama M, Nakayama J, Hidaka H, Honda T, Ishii K, Fukushima M, et al. (2001) Cell lineage specificity of newly raised monoclonal antibodies against gastric mucins in normal, metaplastic, and neoplastic human tissues and their application to pathology diagnosis. Am J Clin Pathol 115:69–79

Ota H, Katsuyama T, Akamatsu T, Fujimori Y, Matsuzawa K, Ishii K, Honda T, et al. (1995) Application of mucin histochemistry for pathological diagnosis—expression of gastric phenotypes in metaplastic and neoplastic lesions and its relation to organoid differentiation. Acta Histochem Cytochem 28:43–53

Ota H, Katsuyama T, Ishii K, Nakayama J, Shiozawa T, Tsukahara Y (1991) A dual staining method for identifying mucins of different gastric epithelial mucous cells. Histochem J 23:22–28

Ota H, Nakayama J, Momose M, Kurihara M, Ishihara K, Hotta K, Katsuyama T (1998) New monoclonal antibodies against gastric gland mucous cell-type mucins: a comparative immunohistochemical study. Histochem Cell Biol 110:113–119

Pereira MB, Dias AJ, Reis CA, Schmitt FC (2001) Immunohistochemical study of the expression of MUC5AC and MUC6 in breast carcinomas and adjacent breast tissues. J Clin Pathol 54:210–213

Reis CA, David L, Carvalh F, Mandel U, de Bolos C, Mirgorodskaya E, Clausen H, et al. (2000) Immunohistochemical study of the expression of MUC6 mucin and co-expression of other secreted mucins (MUC5AC and MUC2) in human gastric carcinomas. J Histochem Cytochem 48:377–388

Rosen SD, Bertozzi CR (1994) The selectins and their ligands. Curr Opin Cell Biol 6:663–673

Sasaki M, Yamato T, Nakanuma Y, Ho SB, Kim YS (1999) Expression of MUC2, MUC5AC and MUC6 apomucins in carcinoma, dysplasia and non-dysplastic epithelia of the gallbladder. Pathol Int 49:38–44

Shimodaira K, Nakayama J, Nakamura N, Hasebe O, Katsuyama T, Fukuda M (1997) Carcinoma-associated expression of core 2 β1,6-N-acetylglucosaminyltransferase gene in human colorectal cancer: role of O-glycans in tumor progression. Cancer Res 57:5201–5206

Suganuma T, Katsuyama T, Tsukahara M, Tatematsu M, Sakakura Y, Murata F (1981) Comparative histochemical study of alimentary tracts with special reference to the mucous neck cells of the stomach. Am J Anat 161:219–238

Terada T, Ohta T, Sasaki M, Nakanuma Y, Kim YS (1996) Expression of MUC apomucins in normal pancreas and pancreatic tumours. J Pathol 180:160–165

Tsutsumi Y, Nagura H, Osamura Y, Watanabe K, Yanaihara N (1984) Histochemical studies of metaplastic lesions in the human gallbladder. Arch Pathol Lab Med 108:917–921

Zhang MX, Nakayama J, Hidaka E, Kubota S, Yan J, Ota H, Fukuda M (2001) Immunohistochemical demonstration of α1,4-N-acetylglucosaminyltransferase that forms GlcNAcα1,4Galβ residues in human gastrointestinal mucosa. J Histochem Cytochem 49:587–596

Induction of peripheral lymph node addressin in human gastric mucosa infected by *Helicobacter pylori*

Motohiro Kobayashi*†, Junya Mitoma*, Naoshi Nakamura‡, Tsutomu Katsuyama§, Jun Nakayama†, and Minoru Fukuda*¶

*Glycobiology Program, Cancer Research Center, The Burnham Institute, La Jolla, CA 92037; and Departments of †Pathology, ‡Internal Medicine, and §Laboratory Medicine, Shinshu University School of Medicine, Matsumoto 390-8621, Japan

Edited by Stuart A. Kornfeld, Washington University School of Medicine, St. Louis, MO, and approved November 9, 2004 (received for review October 9, 2004)

Helicobacter pylori **infects over half the world's population and is a leading cause of peptic ulcer and gastric cancer. *H. pylori* infection results in chronic inflammation of the gastric mucosa, and progression of chronic inflammation leads to glandular atrophy and intestinal metaplasia. However, how this chronic inflammation is induced or maintained is not well known. Here, we show that chronic inflammation caused by *H. pylori* infection is highly correlated with *de novo* synthesis of peripheral lymph node addressin (PNAd) presented on high-endothelial venule (HEV)-like vessels. The number of HEV-like vessels dramatically increases as chronic inflammation progresses. We found that the PNAd is bound by L-selectin·IgM chimeric protein, and decorated by NCC-ST-439 antibody, which is suggested to recognize both nonsulfated and 6-sulfated sialyl Lewis X on core 2 branched O-glycans, and MECA-79 antibody, which reacts with 6-sulfo *N*-acetyllactosamine on extended core 1 O-glycans. These results indicate that PNAd on HEV-like vessels present in the gastric mucosa subsequent to *H. pylori* infection is similar to those on HEVs present in the secondary lymphoid organs, which are essential for lymphocyte circulation. Moreover, eradication of *H. pylori* is associated with the disappearance of HEV-like vessels in the gastric mucosa. By contrast, very few PNAd were found in the gastric mucosa of patients with chemical gastritis caused by nonsteroidal antiinflammatory drugs. These results strongly suggest that PNAd in HEV-like vessels plays a critical role in lymphocyte recruitment during chronic inflammation induced by *H. pylori* infection.**

inflammation | peptic ulcers | gastric carcinoma

Helicobacter pylori is a Gram-negative microaerophilic bacterium that infects >50% of the world's population (1). The infection of *H. pylori* is usually confined to the surface mucous cell-derived mucin (2). If untreated, this infection leads to chronic active gastritis and develops pyloric gland atrophy and intestinal metaplasia expressing intestine-specific genes, including MUC2, sucrase/isomaltase, and carbonic anhydrase 1 (3–7). This second advanced stage of gastritis is closely associated with the pathogenesis of peptic ulcers.

The host responds to *H. pylori* infection primarily by mounting a strong neutrophilic response. Such a response contributes to gastric epithelial damage and is followed by chronic inflammatory infiltrates composed of lymphocytes and plasma cells, forming mucosa-associated lymphoid tissue (8). Although it has not been formally proven, it is suggested that this mucosal inflammation in response to *H. pylori* infection might lead to gastric carcinoma and malignant lymphoma (4, 5, 9–11). It is thus important to understand how lymphocytes are recruited to the gastric mucosa during the progression of chronic inflammation. However, such mechanisms are not fully understood.

In chronic inflammatory states of other systems, L-selectin and its ligands are implicated in lymphocyte recruitment in those diseases for which peripheral lymph node addressin (PNAd) is induced on high-endothelial venule (HEV)-like vessels (12, 13). Such HEV-like vessels have been observed in rheumatoid arthritis, lymphocytic thyroiditis, and inflammatory bowel diseases (14–17). In these studies, the induction of PNAd is detected by MECA-79 antibody (18), which decorates PNAd on HEV-like vessels. Indeed, BCA-1, a homing chemokine in the lymphoid tissue, and MECA-79-positive vessels were detected in mucosa-associated lymphoid tissue associated with *H. pylori* infection (19, 20).

MECA-79$^+$ HEVs in the secondary lymphoid organs play a major role in lymphocyte circulation (12). The MECA-79 epitope has been shown to be 6-sulfo *N*-acetyllactosamine attached to extended core 1 O-glycans, Galβ1→4(SO$_3$→6)GlcNAcβ1→3Galβ1→3GalNAcα1→Ser/Thr (21). Moreover, MECA-79 antibody can also bind to its sialylated and fucosylated form that constitutes PNAd (21). Structural studies also showed that 6-sulfo sialyl Lewis X on core 2 branched O-glycans, sialic acid-α2→3Galβ1→4[Fucα1→3(SO$_3$→6)]GlcNAcβ1→6(Galβ1→3)GalNAcα1→Ser/Thr is present as a major L-selectin ligand on HEVs (21, 22).

In the present study, we found that inflammatory response to *H. pylori* infection is associated with the formation of HEV-like vessels in the gastric mucosa. HEV-like vessels express PNAd, characterized by binding to MECA-79, HECA-452 (23), and NCC-ST-439 (24) antibodies, and L-selectin·IgM chimeric protein. The expression of HEV-like vessels, assessed by MECA-79 and HECA-452 antibody staining, was highly correlated with the degree of lymphocyte infiltration. Moreover, we show that HEV-like vessels disappear once *H. pylori* is eradicated. These results indicate that inflammatory response to *H. pylori* infection is, at least in part, facilitated by induction of PNAd, thereby recruiting lymphocytes to the gastric mucosa.

Materials and Methods

Histological Specimens. We retrieved 143 formalin-fixed, paraffin-embedded blocks of histological specimens with various degrees of chronic gastritis from the archives of the Department of Laboratory Medicine, Shinshu University Hospital. Tissue sections 3 μm thick were stained with hematoxylin and eosin. Based on the updated Sydney system (25), gastritis was evaluated by using a visual analogue scale to evaluate five factors, including (*i*) *H. pylori* density, (*ii*) polymorphonuclear neutrophil activity, (*iii*) chronic infiltration of lymphocytes, (*iv*) glandular atrophy, and (*v*) intestinal metaplasia. Each factor was categorized into four grades: normal, mild, moderate, and marked. This grading

This paper was submitted directly (Track II) to the PNAS office.

Abbreviations: HEV, high-endothelial venule; PNAd, peripheral lymph node addressin; NSAID, nonsteroidal antiinflammatory drug; LSST, L-selectin ligand sulfotransferase; FucT-VII, fucosyltransferase VII; Core1-β3GlcNAcT, core 1 extension β1,3-*N*-acetylglucosaminyltransferase; Core2GlcNAcT-I, core 2 β1,6-*N*-acetylglucosaminyltransferase I; PSGL-1, P-selectin glycoprotein ligand 1.

¶To whom correspondence should be addressed at: The Burnham Institute, 10901 North Torrey Pines Road, La Jolla, CA 92037. E-mail: minoru@burnham.org.

is illustrated in Fig. 6, which is published as supporting information on the PNAS web site.

Biopsy specimens obtained from 20 rheumatoid arthritis patients who had been taking nonsteroidal anti-inflammatory drugs (NSAIDs) were evaluated according to a system (26) modified from Dixon *et al.* (27) for grading of chemical gastritis. Five histological features, which are composed of (*i*) foveolar hyperplasia, (*ii*) edema and prominence of muscle fibers in the lamina propria, (*iii*) vasodilatation and congestion, (*iv*) inverse scale for polymorphonuclear neutrophil activity, and (*v*) inverse scale for chronic lymphocyte infiltration, were graded from 0 (normal or absent) to 3 (marked). Each grade of five categories was added to provide a total chemical score that could range from 0 to 15. Scores from 11 to 15 were considered diagnostic of chemical gastritis. The Ethical Committee of Shinshu University School of Medicine approved these study plans.

Antibodies and Immunohistochemistry. The antibodies used in this study were CSLEX-1 (mouse IgM, Pharmingen), HECA-452 (rat IgM, Pharmingen), MECA-79 (rat IgM, Pharmingen), NCC-ST-439 (mouse IgM, Nippon Kayaku, Tokyo), mouse IgG anti-human CD31 (DAKO), QBEND10 (mouse IgG directed to human CD34, Immunotech, Luminy, France), and rabbit anti-*H. pylori* polyclonal (DAKO). Immunostaining was performed by using the EnVision$^+$ system (DAKO). Briefly, serial sections were deparaffinized and rehydrated, and endogenous peroxidase activity was blocked by soaking in 0.3% H_2O_2 methanol solution. Before immunostaining, the antigens were retrieved by incubating sections in a microwave in 10 mM Tris·HCl buffer (pH 8.0) containing 1 mM EDTA for CD31 and CD34 or by 5 min of treatment with 20 μg/ml proteinase K for *H. pylori*. The tissue sections were blocked with 3% FBS in PBS and incubated with primary antibody. After being washed in PBS, the slides were incubated with horseradish peroxidase- and secondary antibody-conjugated polymer, EnVision$^+$ (DAKO). The color reaction was developed with 3,3′-diaminobenzidine containing 0.02% H_2O_2 (Vector). Sections were briefly counterstained with hematoxylin. Negative controls were obtained by omitting the primary antibodies. Tonsil tissue was used as a positive control (Fig. 7, which is published as supporting information on the PNAS web site).

The numbers of CD34$^+$, MECA-79$^+$, and HECA-452$^+$ vessels in 10 high-power fields of view with ×400 magnification were obtained. The numbers of MECA-79$^+$ and HECA-452$^+$ vessels each were divided by the number of CD34$^+$ vessels, yielding the percentages of MECA-79$^+$ and HECA-452$^+$ vessels, respectively, as described in ref. 28.

Construction of L- and E-Selectin·IgM Chimeras. The Fc region of human IgM was amplified with the oligonucleotides 5′-CGGGATCCTGTGATTGCTGAGCTGCCTCCCA-3′ and 5′-GCTCTAGATCAGTAGCAGGTGCCAGCTGTGT-3′ by using pcDNA1-mouse P-selectin·IgM (29) as a template and subcloned into the *Bam*HI/*Xba*I site of pcDNA1.1 (pcDNA1.1-IgM). For construction of pcDNA1.1-human L-selectin·IgM, the 5′ end of L-selectin was excised from pCDM8-human L-selectin·IgG by *Eco*RI digestion and blunted with Klenow fragment (Roche). After digestion of the 3′ end with *Bam*HI, the excised cDNA was subcloned into the blunted *Hin*dIII site and *Bam*HI site of pcDNA1.1-IgM, to form pcDNA1.1-human L-selectin·IgM. Similarly, the PCR product obtained by using pcDNA1-human E-selectin·IgG (30) as a template, was subcloned into pcDNA1.1-IgM, forming pcDNA1.1-human E-selectin·IgM.

Selectin·IgM Chimeric Protein-Binding Assay. Human L-selectin·IgM and E-selectin·IgM chimeric proteins were obtained from the cultured medium of COS-1 cells after transient transfection of pcDNA1.1-L-selectin·IgM and pcDNA1.1-E-selectin·IgM as described in ref. 31.

After blocking endogenous peroxidase activity as described above, we incubated tissue sections with selectin·IgM chimeric protein and rinsed them with PBS containing Ca^{2+}. The sections were then incubated with horseradish peroxidase-conjugated goat anti-human IgM antibody (Pierce). After being rinsed in PBS containing Ca^{2+}, the color reaction was developed with 3,3′-diaminobenzidine as described above. The sections were briefly counterstained with hematoxylin. A control experiment was done with PBS containing 1 mM EDTA.

Statistical Analysis. The statistical difference in the percentages of positive vessels in different chronic infiltrate grades was analyzed by the Kruskal–Wallis test followed by Dunn's post hoc test. The difference of proportions (percentage of patients) was analyzed by Fisher's exact test. In both tests, P values at <0.05 are considered significant.

Stable Expression of P-Selectin Glycoprotein Ligand 1 (PSGL-1), Fucosyltransferase VII (FucT-VII), Core 1 Extension β1,3-*N*-acetylglucosaminyltransferase (Core1-β3GlcNAcT), Core 2 β1,6-*N*-acetylglucosaminyltransferase I (Core2GlcNAcT-I), and L-Selectin Ligand Sulfotransferase (LSST) in CHO Cells. CHO cells stably expressing PSGL-1 and Core1-β3GlcNAcT, Core2GlcNAcT-I, or FucT-VII were established as described in ref. 32. CHO cells stably expressing PSGL-1, Core1-β3GlcNAcT, and FucT-VII, CHO-PSGL-1·C1·F7 (32) were further stably transfected with pcDNA1.1-LSST (30) and pCMV/Bsd (Invitrogen) and selected with Blasticidin S (Invitrogen). The cells were sorted and cloned for MECA-79$^+$ staining to obtain CHO-PSGL-1·C1·F7·LSST.

CHO-PSGL-1·C2·F7 cells (32) were transfected with pcDNA1.1-LSST. Cloned cells positive for HECA-452 and negative for CSLEX-1 were chosen as CHO-PSGL-1·C2·F7·LSST. Previously, it was shown that 6-sulfo sialyl Lewis X is recognized by HECA-452 antibody but not by CSLEX-1 antibody (33). Similarly, CHO-PSGL-1·C2·F7·LSST cells were stably transfected with Core1-β3GlcNAcT, yielding MECA-79$^+$ CHO-PSGL-1·C1·C2·F7·LSST.

Results

HEV-Like Vessels Are Induced in *H. pylori*-Induced Inflammation. Because it has been reported that *de novo* formation of HEV-like vessels, which express PNAd, is associated with various chronic inflammatory diseases, we determined whether chronic inflammation caused by *H. pylori* infection is also associated with the formation of HEV-like vessels. To do so, gastric mucosa from patients infected with *H. pylori* was stained with MECA-79 antibody, which reacts with 6-sulfo sialyl Lewis X on extended core 1, and HECA-452 antibody, which reacts equally well with sialyl Lewis X and 6-sulfo sialyl Lewis X-capping structure on extended core 1 and core 2 branches (Fig. 1; see also Fig. 8, which is published as supporting information on the PNAS web site). As shown in Fig. 2, gastric mucosa derived from *H. pylori*-infected patients displayed HEV-like vessels expressing MECA-79 and HECA-452 antigens, as well as CD31 and CD34, which are markers for vascular endothelial cells. Moreover, these HEV-like vessels can potentially recruit L-selectin-expressing lymphocytes, because L-selectin·IgM chimeric protein bound the same vessels in a Ca^{2+}-dependent manner. Indeed, a large number of B and T lymphocytes were recruited in the gastric mucosa infected with *H. pylori* (Fig. 9, which is published as supporting information on the PNAS web site). These results indicate that *H. pylori*-induced inflammation is associated with the formation of PNAd present on HEV-like vessels.

The above results demonstrated that 6-sulfo sialyl Lewis X on extended core 1 O-glycans is present based on positive staining by MECA-79 and HECA-452 antibodies. To elaborate further the chemical nature of L-selectin ligands on these HEV-like

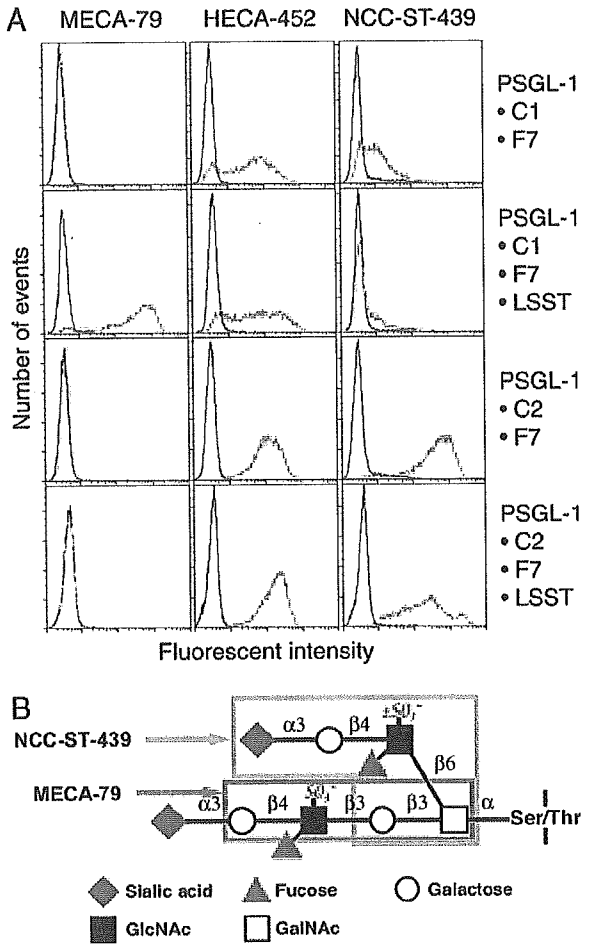

Fig. 1. FACS analysis of transfected CHO cells expressing sialyl Lewis X or 6-sulfo sialyl Lewis X on extended core 1 or core 2 branched O-glycans (32) and structures of MECA-79 and NCC-ST-439 epitopes are shown. (*A*) MECA-79 binds CHO cells expressing 6-sulfo sialyl Lewis X on extended core 1 (CHO-PSGL-1·C1·F7·LSST) but not sialyl Lewis X (CHO-PSGL-1·C1·F7). NCC-ST-439 binds CHO cells expressing sialyl Lewis X (CHO-PSGL-1·C2·F7) and 6-sulfo sialyl Lewis X (CHO-PSGL-1·C2·F7·LSST) on core 2 branched O-glycans but barely binds those expressing sialyl Lewis X or 6-sulfo sialyl Lewis X on extended core 1 O-glycans. HECA-452 binds all cells tested, but its reactivity apparently depends on the expression level of extended core 1 O-glycans. (*B*) L-selectin ligand containing 6-sulfo sialyl Lewis X on core 2 branch and extended core 1 structure is shown. The epitopes for NCC-ST-439 and MECA-79 are shown in boxes.

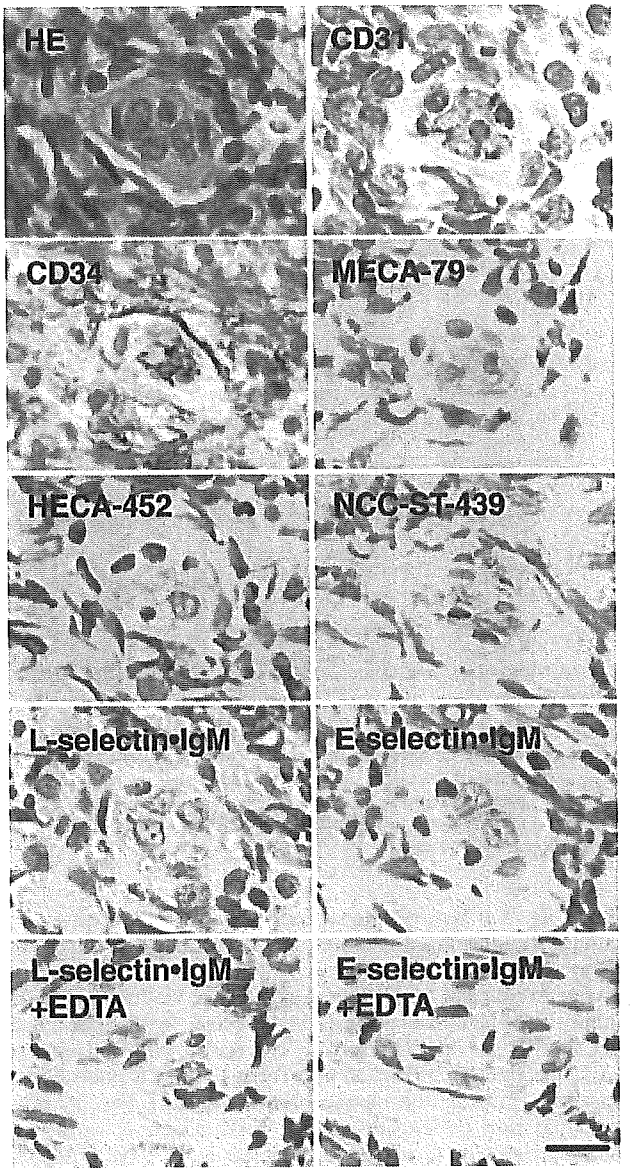

Fig. 2. MECA-79, HECA-452, and NCC-ST-439 antigens in a HEV-like vessel in the gastric mucosa with *H. pylori*-associated chronic active gastritis. Serial sections were subjected to immunostaining with anti-CD31, anti-CD34, MECA-79, HECA-452, and NCC-ST-439 antibodies and to a binding assay with L-selectin·IgM and E-selectin·IgM chimeric proteins in the absence or presence of 1 mM EDTA. HE, hematoxylin and eosin staining. (Bar, 10 μm.)

vessels, the NCC-ST-439 monoclonal antibody was used. NCC-ST-439 antibody binding has been tested for sialyl Lewis X-capping structure on Galβ1→4GlcNAcβ1→6GalNAcα1→R but not on natural core 2 branched O-glycan Galβ1→4GlcNAcβ1→6(**Galβ1→3**)GalNAcα1→R (missing Galβ1→3 shown in bold) (24). Moreover, it has not been determined whether 6-sulfo sialyl Lewis X is also recognized by this antibody. To test these possibilities, we made CHO cells expressing various types of O-glycans and stained the cells with NCC-ST-439 antibody. Fig. 1 illustrates that NCC-ST-439 antibody binds to CHO cells expressing nonsulfated and 6-sulfo sialyl Lewis X on core 2 branched O-glycans but barely to CHO cells expressing those capping structures on extended core 1 O-glycans. Fig. 2 shows that NCC-ST-439 antibody can also stain HEV-like vessels formed in the gastric mucosa. These results combined suggest that PNAd induced by *H. pylori* infection expresses 6-sulfo sialyl Lewis on both extended core 1 and core 2 branched structures in the same manner as PNAd expressed in the secondary lymphoid organs (21).

Increased Formation of HEV-Like Vessels Is Correlated with Progression of Inflammation. Based on morphological examination, progression of inflammation initiated by *H. pylori* infection can be roughly divided into four stages i.e., normal, mild, moderate, and marked (25). In the moderate and marked stages, intestinal metaplasia frequently takes place, which indicates an advanced stage of the disease.

Fig. 3*A Lower* indicates a marked stage of inflammation in which recruitment of mononuclear cells obscured proper glands in gastric mucosa compared with glands shown in mucosa at mild

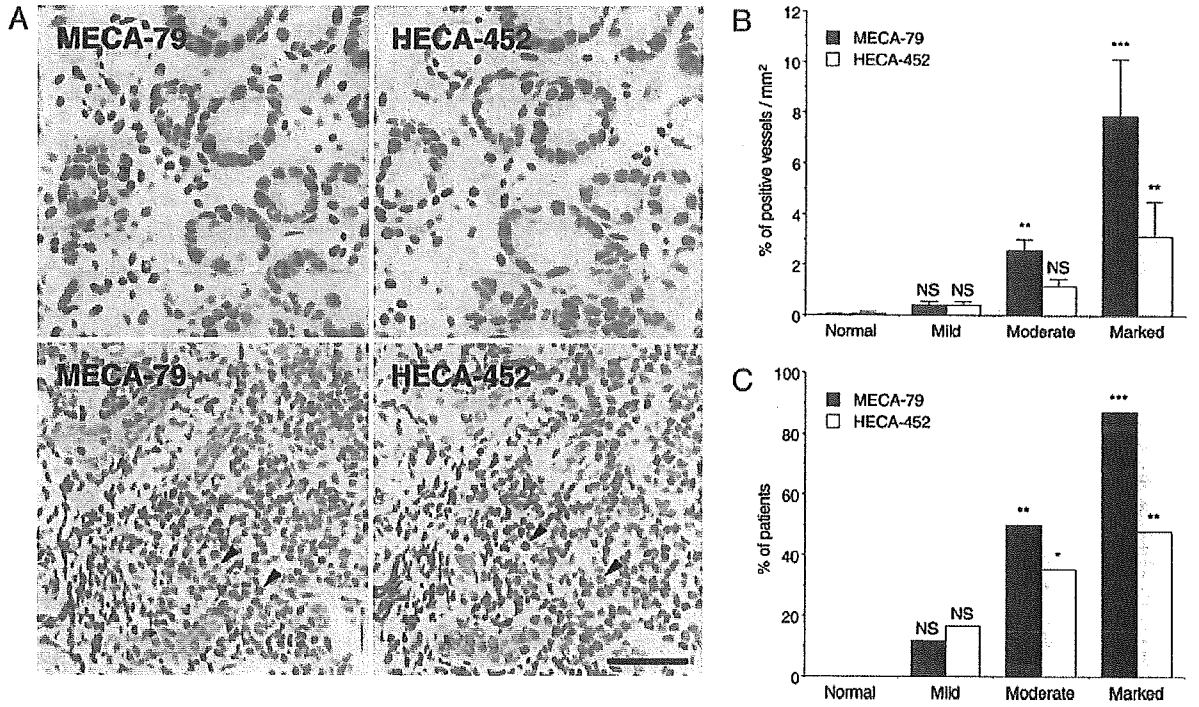

Fig. 3. Gastric mucosa of different degrees of chronic inflammation and association of HEV-like vessels with progression of inflammation. (*A*) (*Upper*) Gastric mucosa at a mild stage barely expresses HEV-like vessels with minimum recruitment of lymphocytes. (*Lower*) Gastric mucosa at a marked stage express a significant number of recruited lymphocytes (arrowheads) around HEV-like vessels. (*B*) The number of MECA-79$^+$ or HECA-452$^+$ vessels is positively correlated with the progression of chronic inflammation. Each group consists of 11 (normal), 42 (mild), 67 (moderate), and 23 (marked) patients. (*C*) The number of patients exhibiting ≥1% MECA-79$^+$ or HECA-452$^+$ vessels is highly correlated with the progression of chronic inflammation. *, $P < 0.05$; **, $P < 0.01$; ***, $P < 0.001$; NS, not significant. (Bar, 50 μm.)

stage (Fig. 3*A Upper*). These observations demonstrate that lymphocyte infiltration is more prominent when HEV-like vessels are more abundant.

After examining >140 human specimens, we found that the number of HEV-like vessels, as detected by MECA-79 or HECA-452 antibody, is positively correlated with the progression of inflammation (Fig. 3*B* and Table 1, which is published as supporting information on the PNAS web site). Fig. 3*C* illustrates that more patients display HEV-like vessels as the inflammation progresses. *H. pylori* was detected in 0%, 21%, 82%, and 87% of patients in normal, mild, moderate, and marked stages of the inflammation, respectively. Overall, HEV-like vessels were found in 79.2% of *H. pylori*-infected patients. These results combined indicate that progression of inflammation, initiated by *H. pylori* infection, is highly correlated with formation of HEV-like vessels at the gastric mucosa.

Formation of HEV-Like Vessels Depends on Continuous *H. pylori* Infection. To determine whether the formation of HEV-like vessels is correlated with the presence of *H. pylori* infection, gastric biopsies were obtained from 17 patients with chronic active gastritis before and after eradication of *H. pylori* by treatment with antibiotics and a proton pump inhibitor. Patients with a moderate inflammation stage displayed both *H. pylori* and HEV-like vessels detected by MECA-79 and HECA-452 antibodies (Fig. 4*A*). After eradication of *H. pylori*, the gastric mucosa of all of the patients examined no longer displayed HEV-like vessels as assessed by MECA-79 and HECA-452 staining and showed minimum lymphocyte infiltration (Fig. 4*B*). These results indicate that continuous infection of *H. pylori* is necessary for formation and maintenance of HEV-like vessels expressing PNAd.

HEV-Like Vessels in NSAIDs-Induced Gastritis. To determine whether HEV-like vessels are induced in chronic inflammatory response by causes other than *H. pylori* infection, gastric mucosa obtained from long-standing rheumatoid arthritis patients taking NSAIDs were examined, because it is known that continuous use of NSAIDs results in chemical gastritis. The majority of 20 patients examined exhibited chemical gastritis phenotype and were devoid of HEV-like vessels (Fig. 5*A*; see also Fig. 10*A*, which is published as supporting information on the PNAS web site). HEV-like vessels were found in the specimens from 6 of 20 patients, but 3 of these patients were also infected with *H. pylori*. All of those three patients display lower scores for chemical gastritis, and HEV-like vessels were likely formed by inflammation caused by *H. pylori* infection. In three *H. pylori*-free patients, HEV-like vessels were found in only 0.68%, 0.67%, and 0.21% of CD34$^+$ vessels, and two of them displayed intestinal metaplasia, suggesting a possible prior infection of *H. pylori*. Fig. 5*B* illustrates that the remaining patient displayed both chemical gastritis phenotype and lymphocyte recruitment. Interestingly, the intensity of MECA-79 staining was much less for this patient than for those infected with *H. pylori* (compare Fig. 5*B* with Figs. 2–4). These results indicate that chemical gastritis negligibly induces PNAd in the gastric mucosa.

Discussion

The present studies demonstrate that *H. pylori*-induced inflammation is associated with the recruitment of lymphocytes through *de novo* formation of PNAd on HEV-like vessels. HEV-like vessels are absent in human gastric mucosa under normal conditions. Once chronic inflammation occurs, these vessels, which bind L-selectin·IgM chimeric protein in a Ca^{2+}-dependent manner, appear. Our observations of *de novo* for-

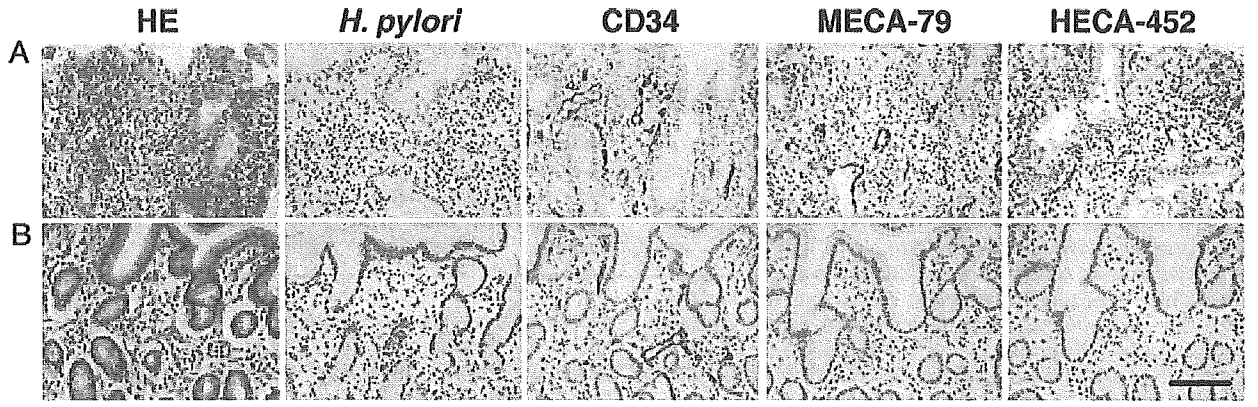

Fig. 4. Disappearance of HEV-like vessels in the gastric mucosa after eradication of *H. pylori*. Gastric mucosa infected by *H. pylori* was examined before and 2 months after a treatment to eradicate *H. pylori*. (*A*) Before the treatment, HEV-like vessels detected by MECA-79 and HECA-452 antibodies were abundant, and large numbers of mononuclear cells (lymphocytes) were present around these vessels. (*B*) After eradication of *H. pylori*, HEV-like vessels were no longer present and few mononuclear cells were present. (Bar, 100 μm.)

mation of HEV-like vessels are similar to those described previously in various human chronic inflammatory diseases, such as rheumatoid arthritis, lymphocytic thyroiditis, inflammatory bowel diseases, and in acute heart allograft rejection (14–17, 34). However, none of the previous studies showed disappearance of HEV-like vessels by removing causes that led to their formation. We have established here that the abundance of HEV-like vessels is highly correlated with the progression of *H. pylori*-associated chronic active gastritis, and that HEV-like vessels are no longer expressed after *H. pylori* is eradicated. By contrast, NSAIDs-induced gastritis patients display only very few HEV-like vessels, if any.

In the present study, we showed that HEV-like vessels are positive for MECA-79 and HECA-452 staining, suggesting that 6-sulfo sialyl Lewis X on the extended core 1 structure is present on PNAd. We also found that HEV-like vessels were stained by NCC-ST-439, the intensity of which was similar to that on neutrophils expressing sialyl Lewis X on core 2 branched O-glycans (35, 36). These results suggest that HEV-like vessels in the gastric mucosa should contain 6-sulfo sialyl Lewis X and sialyl Lewis X on extended core 1 and core 2 branched O-glycans. In previous studies, MECA-79 has been frequently used to characterize PNAd on HEV-like vessels. Although HECA-452 antibody was also used in one study, no structural basis for differential staining was inferred (28). By using HECA-452 and NCC-ST-439 antibodies in addition to MECA-79 antibody, we have obtained more detailed knowledge of the chemical nature of L-selectin ligands on HEV-like vessels induced by *H. pylori* infection. Because it is difficult to isolate a sufficient number of cells expressing PNAd from many pathological specimens, a combination of MECA-79, HECA-452, and NCC-ST-439 staining would be useful to determine the chemical nature of HEV-like vessels formed in these chronic inflammatory diseases.

It has been shown that the *H. pylori* adhesin Sab A binds sialyl dimeric Lewis X-bearing glycosphingolipids in the surface mucous cells (37). The expression of L-selectin ligands including 6-sulfo sialyl Lewis X may thus enhance adhesion of *H. pylori* to mucosa expressing HEV-like vessels. At the same time, colonization of *H. pylori* on the gastric mucosa may contribute to gastritis by producing autoantibodies, because both *H. pylori* and acid-secreting parietal cells share Lewis X antigen (38). Core 2 branched O-glycans are capped by α1,4-linked *N*-acetylglucosamine in the gastric mucosa, and those O-glycans are secreted from gland mucous cells (39). Strikingly, our recent studies demonstrate that this glandular mucin containing α1,4-GlcNAc-capped O-glycans inhibits *H. pylori* growth and thus acts as a natural antibiotic against *H. pylori* infection, whereas MUC5AC secreted from surface mucous cells stimulates *H. pylori* growth

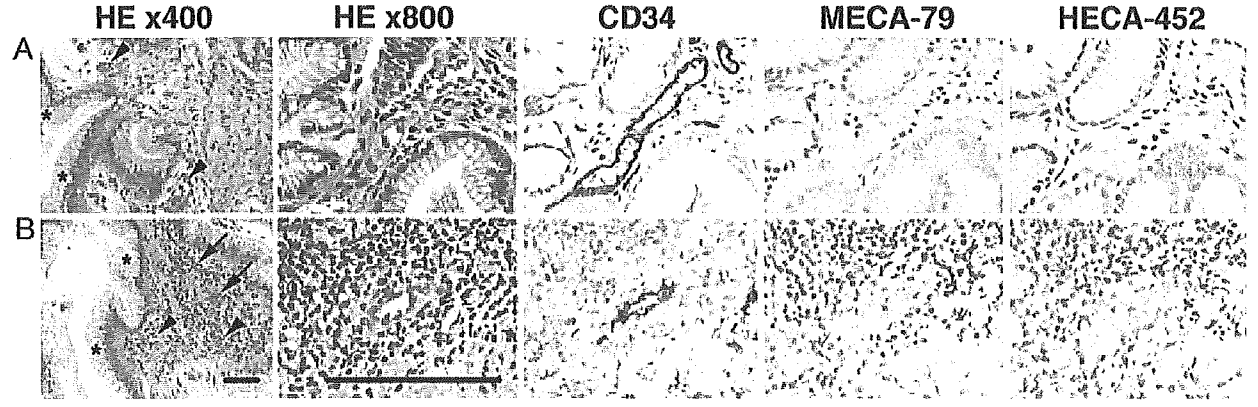

Fig. 5. Few HEV-like vessels are associated with chemical gastritis caused by NSAIDs. (*A* and *B*) Gastric mucosa obtained from two rheumatoid arthritis patients taking NSAIDs. In both patients, typical chemical gastritis phenotype, such as foveolar hyperplasia (asterisks) and vasodilatation and congestion (arrowheads), is evident. (*B*) MECA-79$^+$ HEV-like vessels are associated only with substantial lymphocyte recruitment (arrows), which is rather atypical for chemical gastritis. Images for HE ×800, CD34, MECA-79, and HECA-452 are further enlarged in the same scale to show details. (Bar, 50 μm.)